REVIEW ARTICLE

Cerium Metal-Organic Framework Composites for Supercapacitor Energy Storage

Article history:
Received: 11-10-2023
Revised: 04-11-2023
Accepted: 30-11-2023

Ruhani Baweja[a], Sanjeev Gautam[b], Navdeep Goyal[c]

Abstract: Supercapacitors have emerged as efficient energy storage devices, offering high power density, long cycle life, and rapid charge-discharge capabilities. Advanced materials such as carbon nanotubes (CNTs) and graphene oxide (GO) stand out due to their exceptional electrochemical properties, including open structures and chirality, with capacities ranging from 300 to 1300 mAh g^{-1}. However, the search for cost-effective and highly conductive materials continues to challenge researchers. Metal-Organic Frameworks (MOFs) have surfaced as strong candidates due to their vast surface area, inherent conductivity, and affordability. Nonetheless, the relatively low conductivity of pristine MOFs necessitates composite integration for optimal performance. This review focuses on cerium-based MOF (Ce-MOF) composites, analyzing their structural and electrochemical properties. Key aspects, including synthesis methods, structural characterization, and electrochemical evaluation through cyclic voltammetry and galvanostatic charge-discharge techniques, are discussed in detail. The integration of functional composites into MOFs enhances cycling stability and minimizes capacitance loss over extended use. This review aims to inspire further research into Ce-MOF composites, underscoring their potential as high-performance materials for supercapacitor applications.

Keywords: Metal-organic framework (MOF); CeO_2; Carbon nanotubes (CNTs); Graphene oxide (GO); Capacitance.

1. INTRODUCTION

The escalating global demand for electrical energy has intensified the consumption of fossil fuels and other non-renewable resources, posing critical sustainability challenges. This surge underscores the urgent need to transition toward renewable energy solutions, including solar, wind, and hydroelectric power (Fauzi *et al.*, 2022; Gautam *et al.*, 2023). Advanced methodologies, such as ion implantation (Kaur *et al.*, 2022) and nanomaterial doping (Kaur *et al.*, 2023), have significantly enhanced solar cell efficiency, addressing these growing energy demands. These innovative energy technologies not only offer substantial energy storage capacity but also exhibit robust cyclic performance, making them suitable for diverse applications (Tang *et al.*, 2018).

The growing reliance on energy storage technologies has elevated the importance of batteries, with lithium-ion (Li-ion) batteries emerging as a dominant solution. These batteries have revolutionized portable electronics, electric vehicles, and renewable energy systems through their high energy density and compact designs. A prominent

[a] Department of Physics, Panjab University, Chandigarh - 160 014, India.
[b] Advanced Functional Materials Lab., Dr. S.S. Bhatnagar University Institute of Chemical Engineering & Technology, Panjab University, Chandigarh - 160 014, India.
Corresponding author: sgautam@pu.ac.in
[c] Department of Physics, Panjab University, Chandigarh - 160-014, India.
Corresponding author.

application is the Hybrid Electric Vehicle (HEV), which integrates a battery, an electric motor, and a combustion engine to optimize fuel efficiency (Smith *et al.,* 2010). Despite their widespread adoption, conventional Li-ion batteries face inherent limitations, including restricted power output and finite cycle life (Subramanian *et al.,* 2020). In contrast, supercapacitors have attracted substantial interest as complementary energy storage devices, offering remarkable attributes such as superior power density, rapid charge-discharge rates, and extended operational lifetimes (Wang *et al.,* 2021). They offer a potential alternative to batteries by combining the high specific power of an electrolytic capacitor with the high specific energy of a battery. Supercapacitors store energy primarily in the form of an electrical double layer, enabling them to be recycled millions of times and providing longer lifespans compared to batteries (Nikolaidis *et al.,* 2017).

The increasing demand for energy storage devices with rapid charge-discharge rates and extended cycle lives has spurred interest in advanced capacitors. Supercapacitors stand out as unique energy storage devices, leveraging membranes for ion mobility to achieve superior energy and power densities (Teffu *et al.,* 2021). Their remarkable attributes position them as critical components in applications such as electric vehicles, renewable energy systems, and portable electronics (Ramineni *et al.,* 2022). Despite their promise, enhancing energy and power densities in supercapacitors remains a pivotal challenge tied to the choice of electrode materials. Addressing this, researchers have explored diverse materials—including metal oxides, hydroxides, conducting polymers, ferrites, and sulfides—that exhibit favorable electrochemical properties for use in pseudocapacitors (Tiwari *et al.,* 2020; Sharma *et al.,* 2019).

To enhance electrode efficiency, combining metallic and non-metallic materials with optimized morphologies has proven effective, significantly boosting supercapacitor capacitance (Yuan *et al.,* 2009). For example, reduced graphene oxide (rGO) demonstrates a notable specific capacitance of 684 Fg^{-1} (Padmanathan *et al.,* 2014), which can increase tenfold through platinum (Pt) doping (Cao *et al.,* 2021). Carbon-based materials like graphene and carbon nanotubes (CNTs) are widely used in electric double-layer capacitors (EDLCs) due to their vast surface area, high porosity, and excellent electrical conductivity (Wang *et al.,* 2012). Transition metal oxides such as MnO_2 and NiO_2 offer high capacities, simple synthesis routes, favorable structures, and robust electrochemical properties. However, challenges such as cost, toxicity, limited electrical conductivity, and reduced long-term stability persist, necessitating the search for superior electrode materials (Wang *et al.,* 2019; Prasanna *et al.,* 2015).

Supercapacitors surpass batteries in power density while offering compact size and lightweight designs. Rather than replacing batteries, they complement them, with supercapacitors providing high power output but lower energy-to-weight ratios, while batteries excel in energy storage but deliver lower power levels (Gautham *et al.,* 2019). To address challenges such as low energy density and high self-discharge rates in supercapacitors, materials like carbon-based compounds and conducting polymers are utilized. Conducting polymers, in particular, outperform carbon materials in conductivity, capacitance, and cost-effectiveness. The prevalent n-p polymer configurations enable enhanced energy storage and mechanical robustness. However, limitations such as reduced pseudocapacitor performance in n-doped conducting polymers highlight areas requiring further development (Sharma *et al.,* 2020). To overcome these limitations, researchers are moving towards metal oxides as they show better capacitance than both carbon-based materials and conducting polymer materials (Sharma *et al.,* 2020), and have lower values of equivalent series resistance (ESR).

Some instances of metal oxides are ruthenium, nickel or manganese oxide and among them, manganese oxide is highly preferred because of lower cost. The capacitance and energy density of supercapacitor electrodes can also be improved by methods such as surface modification which includes heteroatom doping and also by compounding with other materials like combining graphene and carbon nanotubes (Bellani *et al.,* 2019). Cong *et al.* developed supercapacitors (SCs) using a combination of graphene and polyaniline (PANI). These SCs exhibited a remarkable capacitance of approximately 763 Fg^{-1} at 1 Ag^{-1} in 1M H_2SO_4, surpassing the capacitance values of the individual components, PANI (520 Fg^{-1}) and graphene (180 Fg^{-1}) (Cong *et al.,* 2013).

Metal-Organic Frameworks (MOFs) have also emerged as highly promising materials for supercapacitor electrodes. Their exceptional properties, such as large surface area, tunable pore sizes, and the incorporation of redox-active metal centers, enable MOFs to exhibit excellent electrochemical performance in supercapacitor devices (Zhao *et al.,*

2016). Furthermore, when employed directly as electrode materials, bare MOFs, with the inclusion of pseudocapacitive redox centers, can provide a greater number of active sites and expedite ion transport between the electrode and electrolyte (Wang *et al.*, 2016). However, the limited flexibility of MOFs and materials derived from them in terms of electrolyte compatibility can lead to reduced stability during the charge/discharge process and this issue has been recognized as a significant limitation in supercapacitor applications (Yang *et al.*, 2014). Fortunately, MOFs can be effectively combined with various other materials, including carbon-based materials, metal nanoparticles, metal oxides, polyoxometalates, and polymers. This integration retains its exceptional attributes of high surface area and pore structure while addressing the issue of low conductivity typically associated with pure MOFs. For instance, Wen *et al.*, introduced a Ni-MOF/CNT composite for supercapacitor applications, achieving an impressive energy density of 36.6 $Whkg^{-1}$ (Wen *et al.*, 2015). In a separate study, Saraf *et al.* investigated the electrochemical characteristics of Cu-MOF combined with reduced graphene oxide (rGO). Their findings highlighted a significant improvement in the capacitance behavior of Cu-MOF and exceptional cyclic stability upon the addition of rGO (Saraf *et al.*, 2016). These combinations of MOFs with carbon materials not only facilitated the efficient utilization of active sites during electrochemical performance but also synergistically enhanced mechanical strength and electrical conductivity.

The combination of MOFs with transition metals such as cobalt, nickel, copper makes it better electrode materials for supercapacitor applications and the specific capacitance obtained for such MOFs ranges from 206.76 Fg^{-1} to 2564 Fg^{-1} (Yang *et al.*, 2017). In comparison to transition metal-containing MOFs, there has been relatively little exploration of lanthanide MOFs as materials for supercapacitor electrodes. To exemplify, Ghosh *et al.* determine the specific capacitance of different lanthanide MOFs like MOF-Ce, MOF-Pr, and MOF-Nd to be 572 Fg^{-1}, 399 Fg^{-1}, and 360 Fg^{-1}, respectively at a current density of 1 Ag^{-1}. This proves Ce-MOF to be a better material for supercapacitor electrodes as it also found to have better retention, which is 81%, after the completion of 5000 cycles, in comparison to other which have 74% and 50%, respectively (Ghosh *et al.*, 2019). Moreover, incorporating metal or metal oxide nanoparticles into MOFs enhances the pseudo-capacitance property of MOFs by augmenting the number of available redox centers. To exemplify, the composite of MOF with ceria, known as cerium oxide metal-organic frameworks (CeO_2-MOFs), has attracted significant attention due to their unique properties and the potential to enhance the efficiency of supercapacitors, as cerium oxide possesses a range of remarkable properties, making it highly versatile and suitable for various industrial applications. These properties include excellent mechanical strength, the ability to exist in different oxidation states, high light transmission, good electrical conductivity, large surface area, high oxygen storage capacity, numerous redox-active sites, and the presence of oxygen vacancies (Xie *et al.*, 2017). These characteristics make cerium oxide a valuable material for electrochemical applications. By leveraging the advantageous characteristics of both cerium oxide and MOFs, MOF/CeO_2 composite offers new opportunities for developing high-performance supercapacitors.

This review delivers a detailed analysis of cerium-based MOF (Ce-MOF) composites, including Ce-MOF/CeO_2, Ce-MOF/GO, and Ce-MOF/CNT, as promising materials for supercapacitors. It highlights the distinctive attributes of cerium and MOFs that drive their demand in energy storage applications. The review examines the synthesis methodologies, structural and electrochemical characterizations, and stability of these composites, offering insights into their potential in advanced energy storage systems. Particular emphasis is placed on the electrochemical properties of Ce-MOF-derived electrodes, including enhancements in capacitance, redox activity, charge storage mechanisms, and long-term stability. Moreover, challenges, optimization strategies, and prospective research directions are discussed to advance the development of Ce-MOF-based supercapacitors. The subsequent sections will delve into the specific aspects of Ce-MOFs and their composites which include Ce-MOF/CeO_2, Ce-MOF/GO, and Ce-MOF/CNT, shedding light on their unique properties, synthesis methods, electrochemical performance, stability, and the path towards optimizing their use in supercapacitor systems to meet present-day requirements.

2. OVERVIEW AND IMPORTANCE

2.1. Supercapacitors

Supercapacitors, also referred to as ultracapacitors or electrochemical capacitors, have emerged

as prominent energy storage devices due to their unique ability to bridge the gap between traditional capacitors and batteries. Their distinctive properties make them suitable for a wide array of applications, ranging from portable electronics to electric vehicles (Iro *et al.*, 2016).

The architecture of a supercapacitor includes two electrodes separated by a permeable membrane, with an electrolyte and current collector facilitating charge storage. Materials with high surface areas are employed to enhance energy storage capacity (Teffu *et al.*, 2021). Unlike batteries, which rely on chemical reactions for energy storage, supercapacitors utilize electrostatic charge mechanisms and electrochemical double-layer capacitance. Based on their charge storage mechanism, supercapacitors are classified into three categories: electric double-layer capacitors (EDLCs), pseudocapacitors, and hybrid capacitors. EDLCs store charge at the inner surfaces of active materials, while pseudocapacitors store energy through redox reactions occurring at the electrode surface (Khan *et al.*, 2021).

Supercapacitors utilize different types of electrolytes, which can be divided into two categories: aprotic and protic electrolytes. Each category offers advantages:

- Protic solvents are water-soluble and considered environmentally friendly. They offer higher conductivity but have a narrow potential window. Examples include sodium hydroxide and sulfuric acid (Libich *et al.*, 2018). These ions have high adsorption ability due to their small size and offer low internal resistance (Abdeladim *et al.*, 2015).
- Aprotic solvents help increase the energy density of supercapacitors by expanding the working voltage window. For example, lithium tetrafluoroborate and lithium perchlorate salts are mixed in organic solvents such as ethylene carbonate and diethyl carbonate (Libich *et al.*, 2018). Since organic ions have larger sizes, their adsorption capability is reduced, which results in higher internal resistance (Abdeladim *et al.*, 2015).
- In conclusion, protic electrolytes with lower resistance have higher power density but lower energy density due to their lower voltage range (Abdeladim *et al.*, 2015).

2.1.1. Electric Double-Layer Capacitors

Electric double-layer capacitors (EDLCs) resemble traditional capacitors in design but differ fundamentally in their charge storage mechanism. Instead of using a dielectric material, EDLCs employ a permeable membrane and an electrode/electrolyte interface to store energy (illustrated in Fig. 1). These capacitors utilize fluid electrolytes, including

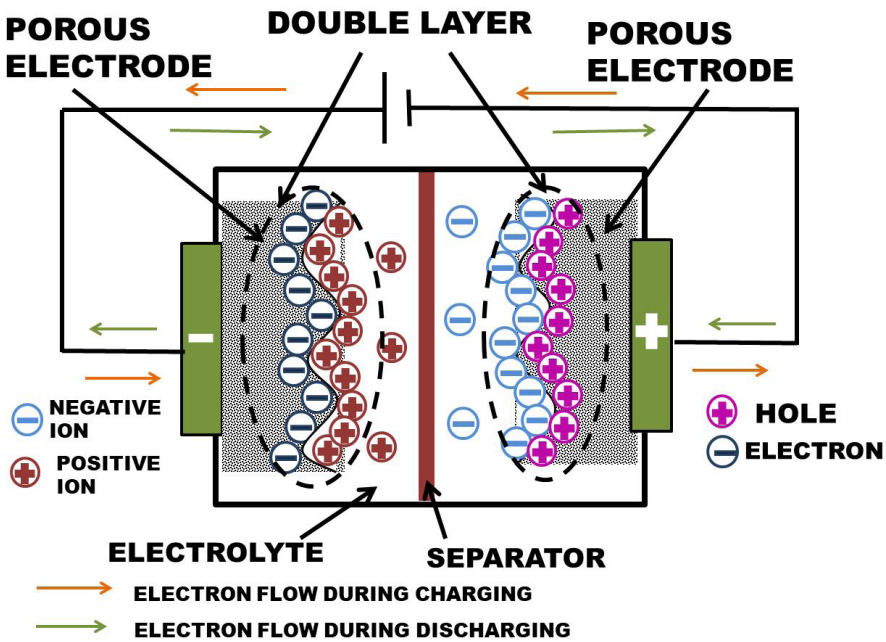

Figure 1. Diagram representing electrical double layer capacitor (Nikolaidis *et al.*, 2017). Adapted with permission under a CCAL from Nikolaidis *et al.*, J. Power Technol., 97, 3, (2017)220-245. Copyright 2017 OJS.

both organic and inorganic options like KOH and H_2SO_4 (Goncalves *et al.*, 2020). The capacitance of EDLCs is influenced by factors such as electrode separation, the choice of electrolyte, and the properties of the separating membrane between the anode and cathode (Ramachandran *et al.*, 2015).

Energy in EDLCs is stored through non-faradaic processes, where double layers form at the electrode/electrolyte interface, accumulating electrostatic charges. The dimensions of these double layers critically affect capacitance. As no chemical reactions are involved, only physical charge-transfer processes occur, ensuring reliable and rapid energy storage (Khan *et al.*, 2021). The behavior of EDLCs is elucidated using three primary models: the Helmholtz model, the Gouy-Chapman model, and the Gouy-Chapman-Stern model, as depicted in Fig. 2. The Helmholtz model describes the formation of an electric double layer, termed the Helmholtz layer, at the electrode-electrolyte interface under an applied electric field. The Gouy-Chapman model extends this by introducing a diffusion layer formed due to the thermal motion of ions. The Stern model integrates aspects of both, dividing the double layer into the stern layer and a diffuse layer.

Within this framework, the inner Helmholtz plane (IHP) is located closer to the electrode surface, while the outer Helmholtz plane (OHP) is farther away, delineating the charge distribution. This combined approach offers a more comprehensive understanding of capacitance in EDLCs (Varghese *et al.*, 2011; Balasubramaniam *et al.*, 2020).

The energy density (E) of electric double-layer capacitors (EDLCs) is determined by the following expression:

$$E = \frac{CV^2}{2.m.3600} \quad (1)$$

where C is capacitance, m is the mass of supercapacitor and V is the region with the maximum value of electrochemical stability.

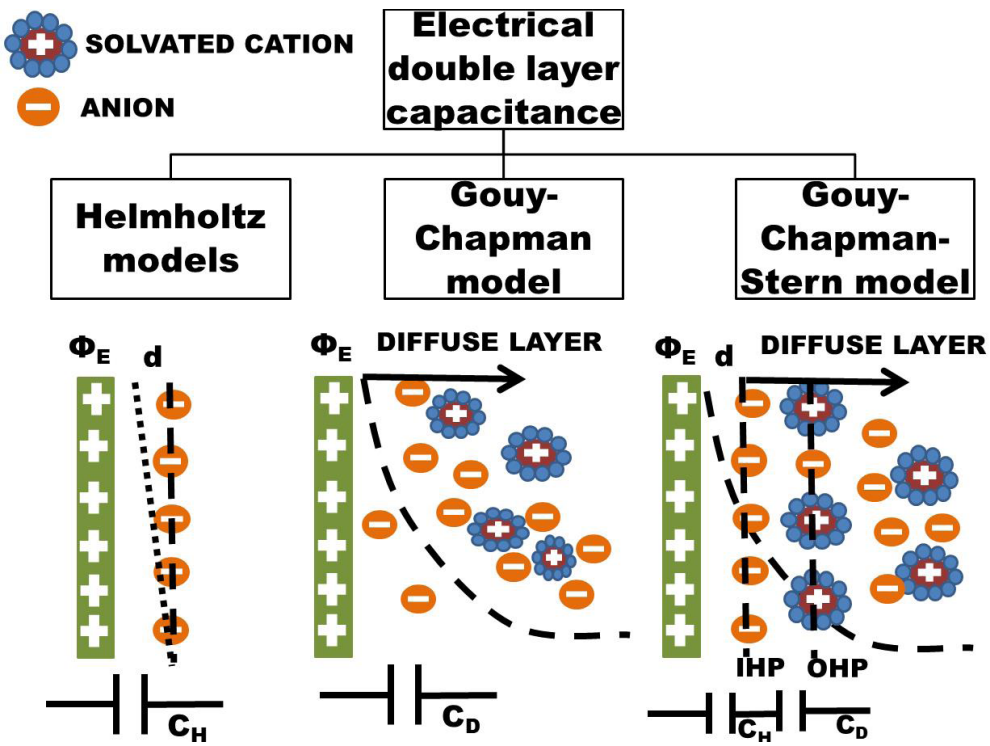

Figure 2. Representation of different models of electrical double layer, shown at positively charged surface (Raza *et al.*, 2018). Adapted from Raza *et al.*, Nano energy, 52(2018). Copyright 2018 Elsevier.

The specific power (P) of a supercapacitor, which reflects its rapid energy delivery capability, is expressed as:

$$P = \frac{V^2}{4.ESR.M} \quad (2)$$

where *ESR* is the equivalent series resistance, a key parameter influencing the power output of the device (Faraji *et al.*, 2015).

2.1.2. Pseudocapacitors

Unlike EDLCs, pseudocapacitors store energy via faradic processes, involving charge transfer between electrodes and electrolytes through oxidation-reduction reactions under an applied potential (Karthikeyan *et al.*, 2021). These electrochemical reactions differ during charge and discharge cycles. Pseudocapacitors typically exhibit energy densities and capacitance values 10 to 100 times greater than EDLCs (Meng *et al.*, 2018). However, their practical application is constrained by lower power densities and reduced cycling stability, which stem from their comparatively weak electrical conductivity (Zhao *et al.*, 2021).

Pseudocapacitance arises from three primary mechanisms: underpotential deposition, redox reactions, and intercalation pseudocapacitance.

- Underpotential Deposition: This occurs when metal ions form a monolayer on the surface of a metal at potentials above their standard redox potential (Augustyn *et al.*, 2014).
- Redox Pseudocapacitance: This involves the physical adsorption of ions onto the material's surface, coupled with faradaic charge transfer (Jiang *et al.*, 2019).
- Intercalation Pseudocapacitance: This mechanism features ion insertion (intercalation) into the electrode material's structure with simultaneous faradaic charge transfer (Djire *et al.*, 2019).

These mechanisms collectively contribute to the enhanced energy storage capabilities of pseudocapacitors.

Hybrid supercapacitors integrate the features of both EDLCs and pseudocapacitors, harnessing the benefits of faradaic and non-faradaic energy storage mechanisms. By combining these processes, hybrid supercapacitors address the limitations of EDLCs (low energy density) and pseudocapacitors (short cycle life), offering enhanced performance in terms of energy and power densities (Lin *et al.*, 2019). The schematic diagram of pseudocapacitors is shown in Fig. 3(a).

Pseudocapacitance can be expressed as:

$$C = \frac{d(\Delta q)}{d(\Delta V)} \quad (3)$$

where (Δq) is the charge acceptance and (ΔV) is the changing potential.

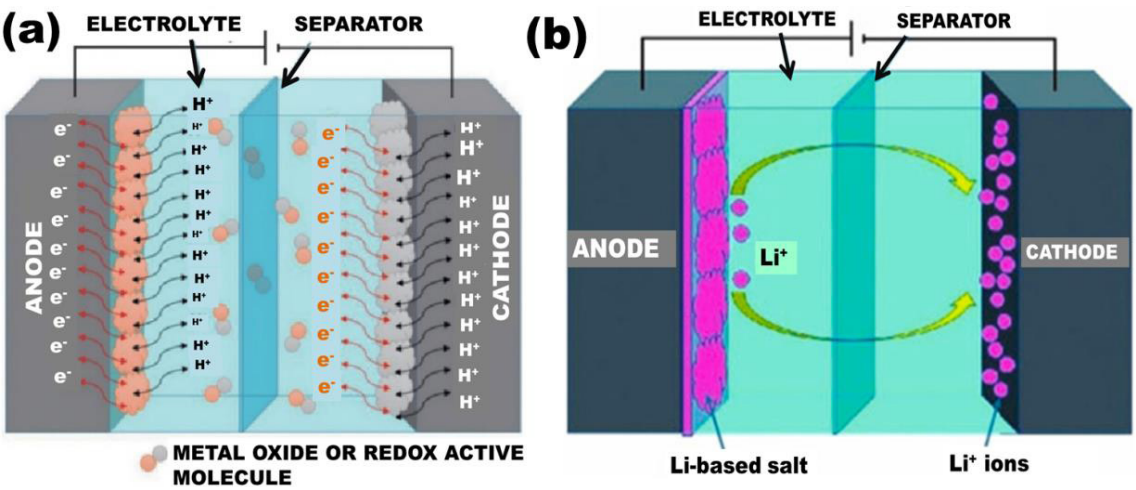

Figure 3. Typical diagram of (a) pseudocapacitor, and (b) hybrid supercapacitor describing flow of charges and ions (Hossain *et al.*, 2020). Adapted from open access under the creative common By license from Hossain *et al.*, Energies, 13 (2020) 14. Copyright 2020 MDPI.

2.1.3. Hybrid Supercapacitors

Hybrid supercapacitors are categorized into three types: composite, asymmetric, and battery-type, as illustrated in Fig. 4.

- Asymmetric Hybrid Supercapacitors: These feature a negative electrode made of carbon materials and a positive electrode composed of pseudoactive materials (Halper *et al.*, 2006).

- Composite-Type Hybrid Supercapacitors: These combine physical and chemical charge storage mechanisms within a single electrode. The integration of carbon-based materials with metal oxides or conducting polymers enhances the surface area and improves electrolyte-pseudoactive material interactions, leading to higher capacitance (Inoue *et al.*, 2007).
- Battery-Type Hybrid Supercapacitors: These incorporate one supercapacitor-like electrode and one battery-like electrode, blending their respective advantages.

These supercapacitors can exist in three forms: composite, asymmetric, and battery- type as shown in Fig. 4. In asymmetric hybrid supercapacitors, the negative electrode is made from carbon materials, while the positive electrode is composed of pseudoactive materials (Halper *et al.*, 2006). Composite-type supercapacitors involve both physical and chemical charge storage mechanisms occurring simultaneously within a single electrode. This is achieved by integrating carbon-based materials with metal oxides or conducting polymers, which increases the surface area and enhances the contact between the electrolyte and pseudoactive material, resulting in higher capacitance (Inoue *et al.*, 2007). In battery-type supercapacitors, one electrode functions as a supercapacitor-type electrode, while the other electrode behaves like a battery- type electrode (Hossain *et al.*, 2020).

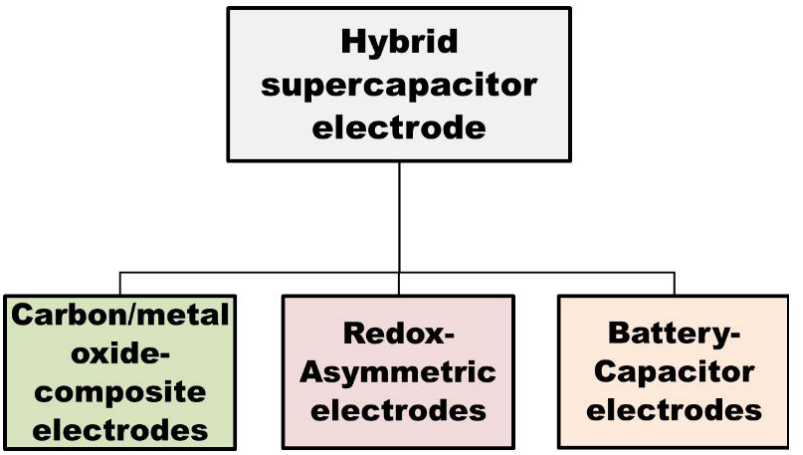

Figure 4. Classification of hybrid electrodes into different types.

The primary difference between symmetric and asymmetric hybrid supercapacitors lies in the composition of their electrodes. Symmetric hybrid supercapacitors use identical materials for both electrodes, typically in hybrid form. In contrast, asymmetric hybrid supercapacitors employ dissimilar materials for the electrodes, allowing for complementary characteristics. Common materials used in asymmetric designs include activated carbon (AC) paired with MnO_2 or AC-$Ni(OH)_2$, optimizing the device's performance through tailored energy and power densities (Muzaffar *et al.*, 2019).

The specific energy (E) of an electrode material is calculated as:

$$E = \frac{C\,\Delta V}{2} \tag{4}$$

where C is the specific capacitance in Fg^{-1}, and ΔV is the cell voltage in volts (Muzaffar *et al.*, 2019).

The power output (P) of a supercapacitor, which indicates its rapid energy delivery capability, is expressed as:

$$P = \frac{E}{t_D} \tag{5}$$

where E represents energy, and t_D denotes the discharge time, equal to t_C (charging time), ensuring Coulombic efficiency through matched charge and discharge densities (Muzaffar *et al.*, 2019).

The specific capacitance (C) of an electrode material is defined as:

$$P = \frac{I}{w \cdot \Delta V} \tag{6}$$

where w is the total electrode mass, I is the average current (A), and ΔV represents the voltage scanning rate (Muzaffar *et al.*, 2019).

3. WHY SUPERCAPACITORS?

The comparative performance of energy storage devices based on energy and power densities is illustrated in Fig. 5. Batteries and capacitors each exhibit unique strengths and limitations: batteries excel in energy storage but deliver lower specific power, whereas capacitors offer exceptional power delivery but have limited energy storage capacity. Supercapacitors bridge this gap by combining high power density with efficient energy storage, making them versatile solutions for a wide range of applications (Li *et al.*, 2022).

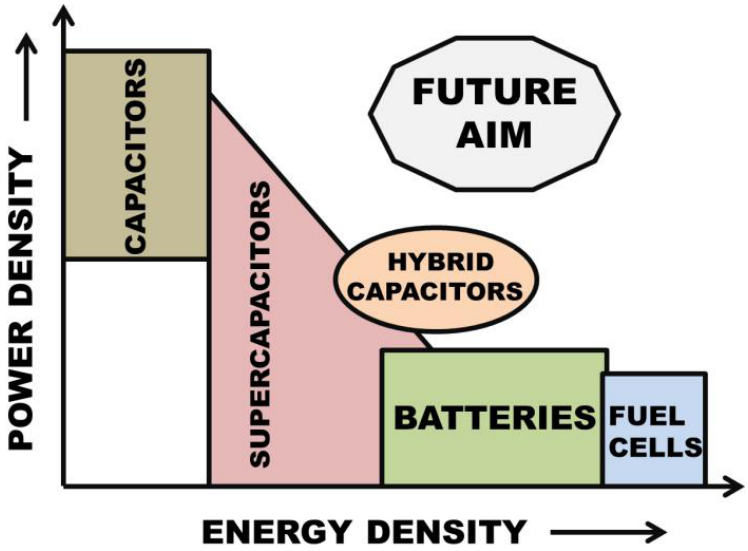

Figure 5. Comparison between energy storage devices on the basis of energy and power density (Riaz *et al.*, 2021). Adapted from open access under the creative common By license from Riaz *et al.*, J. Sens.,21 (2021) 15. Copyright 2021 MDPI.

Supercapacitors are distinguished by their rapid charging capabilities, constrained only by the RC time constant. The charging process follows an exponential curve, whereas discharging occurs almost instantaneously. Unlike batteries, supercapacitors endure unlimited charge-discharge cycles without undergoing chemical reactions, ensuring stable performance over time (Wang *et al.*, 2008).

One of their most notable features is their exceptional cycle life, with the ability to endure hundreds of thousands to millions of cycles with minimal performance degradation. This reliability makes them ideal for long-term applications (Sahin *et al.*, 2022). Additionally, supercapacitors operate efficiently across a broader temperature range than batteries, from +70 °C to -20 °C, as their energy storage mechanism is independent of chemical reactions. However, it is worth noting that extreme temperatures may affect the conductivity of organic electrolytes used in supercapacitors, potentially impacting performance (Green *et al.*, 2002).

3.1. Applications of Supercapacitors

3.1.1. Telecommunication

Supercapacitors play a pivotal role in telecommunications by providing reliable power backup, efficient energy management, and operational stability. During power outages or interruptions, supercapacitors discharge stored energy rapidly, ensuring seamless operation of critical systems, including data centers, network routers, and communication infrastructure. Their high power density makes them ideal for delivering short-term backup power until secondary sources, such as generators or batteries, become active. Furthermore, their compact design makes them well-suited for space-constrained telecommunication systems and equipment (Abdeladim *et al.*, 2015).

3.1.2. Transportation - Electric Vehicle

Supercapacitors are integral to modern transportation, particularly in electric vehicles (EVs) and

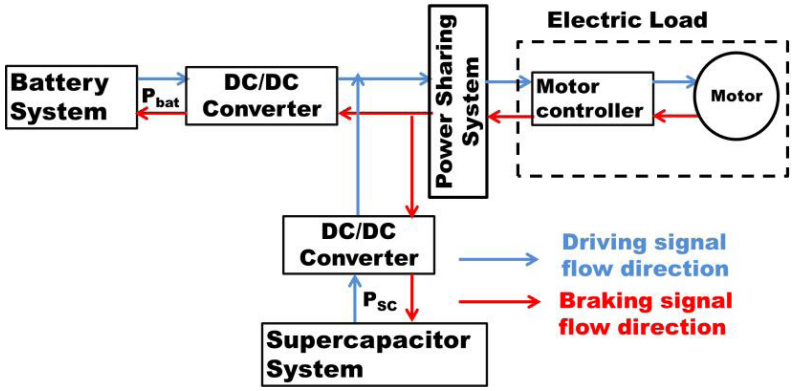

Figure 6. Use of supercapacitors in hybrid electric vehicles for compensating the requirement of rapid acceleration and deceleration (Zhang *et al.,* 2016). Adapted with permission under an CC by 4.0 from Zhang *et al.,* Energies, 9, 5 (2016). Copyright 2016 MDPI.

hybrid electric vehicles (HEVs). In HEVs, supercapacitors address the need for rapid power bursts during acceleration and deceleration while effectively capturing and storing energy during regenerative braking. Their ability to charge and discharge swiftly makes them indispensable for delivering instantaneous power during acceleration and recovering energy during braking, as illustrated in Fig. 6.

By incorporating supercapacitors into HEV systems, overall vehicle performance and energy efficiency are significantly improved. Moreover, their integration with batteries reduces the stress on battery systems by supplying transient currents, thereby prolonging battery life. This capability enhances the overall energy efficiency of vehicles and makes supercapacitors particularly valuable for optimizing regenerative braking systems (Shah *et al.*, 2008).

3.1.3. Renewable energy systems

Supercapacitors are instrumental in renewable energy systems, addressing challenges associated with surplus energy storage and compensating for the intermittent nature of solar and wind power. They mitigate power fluctuations and provide short-term energy storage, enhancing grid stability and integration. By managing peak power demands and balancing loads on the grid, supercapacitors alleviate the strain on primary energy sources during high-demand periods by discharging stored energy rapidly.

Additionally, supercapacitors enable efficient energy time-shifting, storing excess energy generated during low-demand periods and releasing it when demand rises. This capability optimizes energy utilization, reduces reliance on conventional power plants, and supports a more sustainable and efficient energy framework (Van Voorden *et al.*, 2007; Sahin *et al.*, 2022).

4. EFFICIENT MATERIALS IN SUPERCAPACITORS

Efficient materials play a critical role in enhancing the performance of supercapacitors by improving key parameters such as energy density, power density, cycle life, and internal resistance. Various materials including metal oxides, conductive polymers, and carbon-based materials, have demonstrated their potential as efficient choices. Materials with high specific capacitance enable supercapacitors to store more energy per unit mass or volume, resulting in higher energy storage capacity. For example, spinel ferrite nanomaterials exhibit excellent capacitance, durability, and long-term stability, making them desirable electrode materials for supercapacitors (Elkholy *et al.*, 2017). Graphene, with its unique properties, can also enhance the energy density of supercapacitors by carefully balancing the mass and amounts of positive and negative electrodes (Redondo *et al.*, 2020).

Materials that facilitate fast ion transport and charge transfer kinetics can enhance the power density of supercapacitors and enable rapid charging and discharging rates. For instance, N-doped graphene hydrogel, synthesized through the hydrothermal process, demonstrates an outstanding power density of 205 kW kg^{-1} (Abdel *et al.*, 2021). Carbon-based materials, known for their durable power density, also contribute to efficient energy storage (Abdel *et al.*, 2021).

Materials with high stability and resistance to degradation are crucial for ensuring the long cycle life of supercapacitors. Carbon-based materials, known for their excellent cycle stability, are widely utilized. Additionally, polymer-based materials are gaining importance due to their remarkable properties such as flexibility, conductivity, and ease of synthesis (Snook *et al.*, 2011). Materials with lower values of electrical resistance can minimize the energy losses during the charging and discharging processes, resulting in higher overall energy conversion efficiency. For example, the specific capacitance of a $ZnCo_2S_4$ electrode is approximately four times higher than that of a Zn-Co electrode due to its low charge transfer resistance, resulting in improved energy storage performance (Li *et al.*, 2019).

A range of metal oxides, including RuO_2, MnO_2, NiO, Fe_3O_4, ZnO, TiO_2, and others, have been investigated as potential electrode materials for supercapacitors. These active materials, when carefully integrated into the graphene structure in specific proportions, can yield exceptional electrode materials. The incorporation of metal oxide nanoparticles serves as nanoscale spacers between the layers of graphene, effectively preventing them from re-stacking. In their study, Lu *et al.* have explored the supercapacitor properties of composite materials comprising graphene and either ZnO or SnO_2. Their findings reveal a notable enhancement in the electrochemical performance of graphene-ZnO composites when compared to pristine ZnO, SnO_2, or graphene. Specifically, the graphene-ZnO composite exhibited a significantly improved capacitance value and reversibility. It achieved a specific capacitance of 61 Fg^{-1} and an energy density of 4.8 $Whkg^{-1}$, surpassing the corresponding values for graphene-SnO_2 samples (Lu *et al.*, 2010). Additionally, the authors investigated a graphene-MnO_2 composite with a high MnO_2 content of 78 wt.%. This composite exhibited a remarkable specific capacitance of 310 Fg^{-1} at a scan rate of 2 mVs^{-1}. The authors attributed this impressive performance to the synergistic effect of graphene and MnO_2, which increased the specific surface area, resulting in enhanced conductivity and ultimately yielding a high-performance supercapacitor (Yan *et al.*, 2010). Composites formed by combining graphene with electrically conductive polymers such as polyaniline, polythiophene, polypyrrole, and poly(3,4-ethylenedioxythiophene) have garnered significant attention. The combination of the inherent flexibility and electrical conductivity of these polymers with graphene's layered structure makes for a promising material suitable for electrode applications in supercapacitors. The growing demand for lightweight, flexible, and smaller supercapacitors in the field of future electronics has sparked a keen interest in these graphene/polymer composite electrodes. Notably, these composites exhibit enhanced mechanical strength and conductivity when compared to each individual material. As an illustration, the composite of graphene and polyaniline nanorods demonstrated an impressive specific capacitance of 555 Fg^{-1} when tested in a 1 M H_2SO_4 electrolyte, and it exhibited remarkable cyclic stability over 2000 cycles (Xu *et al.*, 2010).

Li *et al.* synthesized a flexible, lightweight, self-standing film by combining activated carbon, CNT (carbon nanotubes), and reduced graphene oxide (rGO) (Li *et al.*, 2018). This hybrid film weaves a 3D porous framework using CNTs and graphene, which accommodates activated carbon particles through van der Waals forces. In this material, each component plays a vital role: carbon particles prevent graphene restacking, and CNTs enhance electronic conductivity. The resulting AC/CNT/rGO electrode displayed a specific capacitance of 101 Fg^{-1} in an organic electrolyte at the current density of 0.2 Ag^{-1}, and with a maximum energy density of 30 $Whkg^{-1}$. Notably, this flexible hybrid film can operate over a wide temperature range, from -40°C to 200°C. The electrode material exhibited a maximum area-specific capacitance of 330 $mFcm^{-2}$, an energy density of 1.7 $mWhcm^{-3}$, and maintained 90% retention even after 100,000 cycles (Zang *et al.*, 2017).

Some metal oxides have been investigated as an electrode material because of their lower cost and good electrical conductivity. Magnetite-carbon composites have been explored as electrode materials in energy storage devices because of their cost-effectiveness and relatively strong reversible redox activity. These electrode composites demonstrate specific capacitances ranging from 115 to 220 Fg^{-1}, coupled with excellent cyclic stability (Sinan *et al.*, 2016). Guan *et al.* reported the creation of a Fe_3O_4-CNT composite supercapacitor electrode using a straightforward hydrothermal treatment process. This electrode exhibited a specific capacitance of 117 Fg^{-1} and achieved a maximum energy density of 16 $Whkg^{-1}$ (Yang *et al.*, 2014). Similarly, in a comparable approach, substituting CNTs with RGO (reduced graphene oxide) resulted in improved electrochemical performance for the Fe_3O_4-RGO composite. In this particular study,

the Fe_3O_4-RGO composite displayed a notably high specific capacitance of 220 Fg^{-1}, which maintained its stability even after 3000 charge/discharge cycles (Wang *et al.*, 2014).

Metal-organic frameworks possess structured cavities within the organic ligand coordination network, allowing for the attainment of a surface area spanning several thousand square meters per gram. The metal ions present in MOFs may undergo reversible redox interactions making it a desirable candidate for energy storage, especially in supercapacitors. However, they possess some lesser conductivity and thus are combined with various composites to ensure high specific capacity, good electron accessibility and long-term mechanical and electrochemical stability (Lee *et al.*, 2012). For instance, Fleker *et al.* synthesized hybrid compositions of MOF-activated carbon, where the activated carbon functions as the conducting host for MOF nanoparticles. The MOF's precursor materials were introduced into the pores of the activated carbon, and the MOFs were then synthesized within these nanopores (Fleker *et al.*, 2016). Intriguingly, an electron paramagnetic resonance (EPR) signal indicated that MOF nanoparticles in contact with activated carbon exhibited electron-conductive behavior. Moreover, the Cu^{2+}/Cu^{+} redox couple within the MOF contributed a 30% capacity increase to the double-layer capacitance of the activated carbon. Yaghi *et al.* extensively explored the growth of MOFs on graphene substrates. They investigated the electrochemical performance of a comprehensive series of 23 distinct MOFs featuring diverse organic functionalities, metal ions, pore sizes, shapes, and structure types. The graphene sheets served as a conductive platform for the active MOF materials. Several MOFs displayed exceptional performance, with the highest areal capacitance recorded at 5.09 $mFcm^{-2}$, achieved by a zirconium-based MOF over 10,000 charge/discharge cycles (Choi *et al.*, 2014).

4.1. Metal organic Framework (MOFs)

4.1.1. What are MOFs?

Metal-Organic Frameworks (MOFs) are porous crystalline materials characterized by large surface areas and adjustable pore sizes, achieved through the modification of organic ligands that coordinate with metal ions (Xu *et al.*, 2020). These properties endow MOFs with exceptional versatility, making them valuable in various applications such as catalysis, drug delivery, and energy storage (Sangeetha *et al.*, 2020). Their well-ordered porous structures allow for the encapsulation and stabilization of nanomaterials within their networks. MOFs exhibit diverse structural configurations, including 0D, 1D, 2D, and 3D forms, as illustrated in Fig. 7. These structures are created by the coordination of metal ions with organic ligands, resulting in distinct pore types: micropores, mesopores, and macropores. A significant advantage of MOFs is their ability to combine mesoporous and microporous structures within a single framework, enhancing their functionality across various applications (Hassan *et al.*, 2020; Hou *et al.*, 2020).

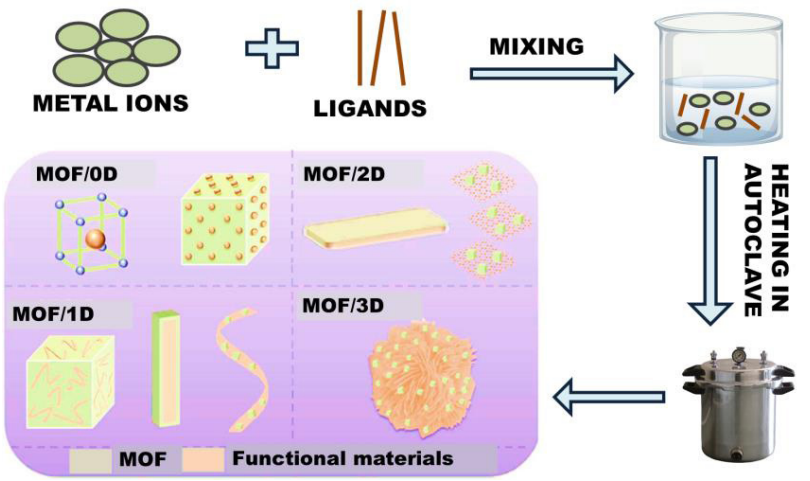

Figure 7. The process describing the formation of metal organic framework (Javed *et al.*, 2023). Adapted with permission under an CC BY-NC 3.0 from Javed *et al.*, RSC advances, 13, 2 (2023). Copyright 2023 Royal Society of Chemistry.

MOFs have recently emerged as promising candidates for energy storage and conversion, particularly in supercapacitor applications. Some MOFs, classified as pseudocapacitors, combine high surface area, tunable porosity, and intrinsic electrochemical activity, making them ideal for improving the energy storage capabilities of supercapacitors (Cao *et al.*, 2022). MOFs are increasingly replacing carbon-based materials such as carbon nanotubes (CNTs) due to their cost-effectiveness and comparable specific capacitance. Their exceptional properties make MOFs highly desirable for supercapacitor applications, where they can be employed directly or as components in advanced composite materials (Khan *et al.*, 2021).

4.2. Synthesis of MOFs

MOF synthesis typically involves the coordination of metal ions or clusters with organic ligands under controlled reaction conditions. Common methods include hydrothermal and solvothermal techniques, which utilize high temperatures and pressures in autoclaves. These processes facilitate the dissolution of otherwise insoluble elements, ensuring efficient and energy-saving synthesis (Cao *et al.*, 2022).

Mechanochemical synthesis offers a solvent-free alternative for MOF production, relying on mechanical forces like grinding or milling to trigger reactions between metal precursors and organic linkers. This method boasts several benefits, including reduced reaction times, enhanced product purity, and alignment with green chemistry principles (Raptopoulou *et al.*, 2021). Additionally, metal oxides are often used as starting materials instead of metal salts in this method, as water is produced as a by-product by using metal oxides.

Sample	Electrode	Surface area	Electrolyte	Current density Ag^{-1}	Capacity	References
C-MOF-2	Negative	1378	1M H_2SO_4	1	170 Cg^{-1}	(Aiyappa *et al.*, 2013)
Co-MOF	Positive	2900	1M LiOH	0.6	103 Cg^{-1}	(Diaz *et al.*, 2012)
MOF-Co_9S_8	Positive		3M KOH	1	1252 Cg^{-1}	(Yang *et al.*, 2020)
MOF-$Ni_xCo_{3-x}O_4$	Positive		3M KOH	1	1291 Cg^{-1}	(Jayakumar *et al.*, 2017)
MOF-NiS	Positive		2M KOH	1	744 Cg^{-1}	(Qu *et al.*, 2018)
Ni-MOF	Positive		2M KOH	1	726 Fg^{-1}	(Kang *et al.*, 2014)
Tb-MOF	Positive		6M KOH	1	510 Fg^{-1}	(Jafari *et al.*, 2020)
Eu-MOF	Positive		6M KOH	1	468 Fg^{-1}	(Dezfuli *et al.*, 2019)
NiCo-MOF	Positive		2M KOH	1	1202.1 Fg^{-1}	(Wang *et al.*, 2019)
Ni-MOF/CNTs	Positive		6M KOH	0.5	1765 Fg^{-1}	(Wen *et al.*, 2015)

Table 1. Some electrodes made using MOF composites for the supercapacitors.

Another important method for MOF synthesis is the microwave-assisted technique. This technique aids in the formation of nanoporous materials with high crystallinity. It allows for the selection of specific structures and results in a narrow particle size distribution (Stock *et al.*, 2012). The synthesis of MOFs can be influenced by various factors, including pH, temperature, reactant concentration, and reaction time. These parameters need to be carefully controlled to achieve the desired structure and properties of the MOF.

Following MOF synthesis, comprehensive characterization is essential to evaluate crystal structure, morphology, surface area, and porosity. Techniques such as X-ray diffraction (XRD), scanning electron microscopy (SEM), transmission electron

microscopy (TEM), and nitrogen adsorption-desorption (BET analysis) are commonly employed to obtain detailed insights into the properties and quality of the synthesized MOFs.

4.3. Properties and characteristics of MOFs

Metal-Organic Frameworks (MOFs) showcase a diverse range of properties owing to their unique architecture, which combines inorganic metal nodes or clusters with organic linkers. A defining characteristic of MOFs is their exceptionally high surface area, often surpassing thousands of square meters per gram. This property, derived from their porous nature, makes MOFs ideal for the adsorption and storage of gases and molecules. The porosity and pore size distribution in MOFs can be finely tuned through the careful selection of metal nodes and organic linkers. This adaptability enables the design of MOFs with customized properties, making them suitable for accommodating specific guest molecules and optimizing performance across various applications (Raptopoulou *et al*., 2021).

The exceptional characteristics of MOFs make them highly suitable for use as electrode materials in supercapacitors. The abundance of surface pores in MOF electrodes facilitates effective electrolyte penetration, promoting enhanced faradaic redox reactions. This results in improved specific capacitance and boosts the overall performance of energy storage devices (Javed *et al.,* 2018). Table 1 summarizes the variations in capacitance performance of supercapacitors employing different MOF materials under varying current densities.

MOFs' distinctive structural features also make them suitable for selective sensing applications. Guest molecules interacting with the MOF framework can alter its electrical, optical, or magnetic properties, enabling precise detection. These attributes make MOFs ideal for sensing applications in environmental monitoring, healthcare diagnostics, and security (Jiao *et al*., 2019).

4.4. Applications of MOFs in energy storage

Metal-Organic Frameworks (MOFs) have attracted considerable interest in energy storage applications, primarily due to their unique features, including high surface area, tunable porosity, and multifunctionality. These properties make MOFs ideal candidates for various energy storage technologies such as gas storage, hydrogen storage, battery electrodes, and supercapacitors. In battery technology, MOFs have shown significant potential as electrode materials in both lithium-ion batteries (LIBs) and alternative battery systems. Their tunable structure enables the development of electrodes with tailored properties, including high specific capacity, superior rate performance, substantial lithium storage capacity, and extended cycle life. MOFs can serve as active electrode materials, conductive additives, or protective coatings, enhancing both the performance and stability of batteries.

One notable advantage of employing MOFs as cathode materials is their ability to endure high current densities without significant structural degradation (De Combarieu *et al*., 2009). Additionally, MOFs demonstrate good performance as anode materials (Song *et al*., 2016). Figure 8 illustrates the mechanisms of energy storage across various devices, highlighting the specific types of MOFs suited for each application. Although advantageous, MOF films on substrates often encounter challenges such as incomplete coverage and poor adhesion, which can undermine structural integrity and electrode performance. Irregular film growth can result in gaps and defects, adversely affecting electrochemical properties and long-term stability. Furthermore, weak adhesion of MOF films may lead to detachment or delamination during battery operation, causing active material loss and diminished electrode efficiency.

MOFs are gaining popularity in supercapacitor applications due to their high surface area, adjustable porosity, and inherent electrochemical activity. These characteristics enable MOFs to be used as standalone electrode materials or in combination with other substances to boost performance. For instance, composites of MOFs with conductive carbon materials, such as graphene or carbon nanotubes (CNTs), demonstrate enhanced specific capacitance and improved stability. However, the limited cyclic stability of pristine MOFs remains a significant challenge (Song *et al*., 2011). To address the limitations of pristine MOFs, hybrid composites have been developed by integrating MOFs with materials that provide enhanced conductivity and stability. For instance, reduced graphene oxide (rGO) is frequently incorporated into MOFs to improve their electrical conductivity and cyclic performance. Likewise, the combination of Ni-MOF with CNTs has demonstrated potential in asymmetric

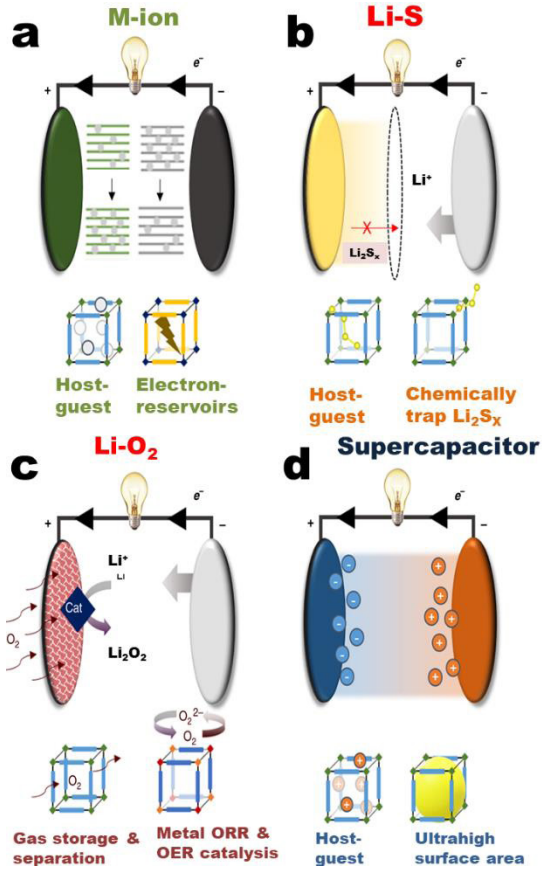

Figure 8. Typical energy storage devices and the mechanisms by which energy is stored, which further characterizes the type of MOF required (a) Metal-ion batteries, (b) Lithium-sulfur batteries, (c) Lithium-oxygen batteries, and (d) Supercapacitors (Baumann *et al.,* 2019). Adapted with permission under an CC by 4.0 from Baumann *et al.,* Communications Chemistry, 2, 1 (2019). Copyright 2019 Nature Publishing Group UK London.

supercapacitors by leveraging the complementary properties of both materials. Figure 9 illustrates the performance of various MOF-based composites in supercapacitor applications (Lu *et al*., 2012).

To address these challenges, researchers are exploring strategies to improve the growth and adhesion of MOF films on substrates. Approaches such as substrate surface modification, the use of adhesion-promoting layers, and the optimization of film deposition methods are being developed to ensure uniform growth and robust substrate interactions. Additionally, scalable fabrication techniques for MOF-based electrodes with high surface area and enhanced conductivity are under investigation to meet the growing demand for efficient energy storage devices (Baumann *et al*., 2019). Sodium-ion batteries have gained considerable attention as a cost-effective alternative to lithium-ion batteries, owing to the abundance and affordability of sodium resources. While their operational principles are similar to those of lithium-ion batteries, the larger size and higher atomic mass of sodium ions result in slower insertion and extraction rates. This has driven research into materials with larger tunnel structures to enable faster sodium-ion transport (Mehtab *et al*., 2019). The stability and tunability of MOFs make them excellent candidates for accommodating larger sodium ions, effectively addressing the limitations of slower ion kinetics. The versatility of MOFs makes them highly adaptable materials for a variety of energy storage applications, particularly in supercapacitors and batteries. However, limitations such as low electrical conductivity and reduced cyclic stability remain critical barriers to their widespread adoption. Addressing these challenges requires innovative approaches, such as scalable synthesis methods and the development of hybrid materials, to unlock their full potential.

One promising strategy involves the integration of conductive polymers, such as polyaniline and polypyrrole, into MOF structures. This hybridization enhances the electrochemical properties of MOFs by combining the conductivity and flexibility of polymers with the porosity and structural precision of MOFs. MOF-polymer composites demonstrate improved charge storage capacity, cyclic stability, and rate performance, positioning them as strong candidates for next-generation energy storage systems (Li *et al.*, 2021).

MOFs are also increasingly utilized in supercapacitor electrodes due to their exceptional properties, such as high surface area and tunable pore sizes. While they can be employed directly, composite approaches are often necessary to overcome limitations in cyclic stability. Hybridizing MOFs with materials like graphene and carbon nanotubes significantly enhances their electrochemical performance, ensuring better conductivity and stability during charge-discharge processes (Khan *et al.*, 2021).

In addition, functionalized MOFs with modified organic linkers, such as hydroxyl (-OH), carboxyl (-COOH), and amino ($-NH_2$), further improve MOF-electrolyte interactions. These functional groups enhance redox activity and ion transport, resulting in significantly higher capacitance and energy density compared to unmodified MOFs (Li *et al.*, 2014). Similarly, combining MOFs, such as Ni-MOF, with carbon nanotubes has shown considerable potential in asymmetric supercapacitors, leveraging the complementary properties of both materials (Wen *et al.*, 2015).

MOFs are also valuable as templates or precursors for the synthesis of porous carbon, metal sulfides, and oxides, which can be used as high-performance supercapacitor electrodes. MOF-derived porous carbon, in particular, exhibits excellent electrochemical performance due to its high mesoporosity and conductivity. These advances highlight the superior electrochemical performance of MOFs and MOF-based materials, making them promising and stable options for energy storage technologies.

While MOFs hold great promise, further research is essential to overcome challenges such as low conductivity and limited stability under harsh conditions. Efforts are focused on hybridizing MOFs with conductive materials, functionalizing linkers to improve electrochemical behavior, and employing structural engineering to enhance their mechanical and chemical resilience. These advancements will be critical in expanding the practical applications of MOFs in energy storage systems (Wang *et al.*, 2015).

4.5. Ce-MOFs: Electrifying Supercapacitor Performance

Cerium-based metal-organic frameworks (Ce-MOFs) have emerged as exceptional materials for supercapacitor applications, owing to their high surface area, tunable porosity, and intrinsic redox-active sites. These properties enable Ce-MOFs to significantly enhance both the energy density and power density of supercapacitors. Additionally, the redox-active cerium ions (Ce^{3+}/Ce^{4+}) provide a notable advantage for faradaic charge storage, resulting in higher specific capacitance compared to traditional electrode materials (Montini *et al.*, 2016).

Ce-MOFs are predominantly synthesized using solvothermal or hydrothermal methods, wherein cerium salts react with organic linkers under controlled temperature and pressure. This process yields highly crystalline frameworks with well-defined porous architectures (He *et al.*, 2020). To address the inherent low electrical conductivity of MOFs, they are often hybridized with conductive materials such as graphene, reduced graphene oxide (rGO), or carbon nanotubes (CNTs). These hybrid composites exhibit significantly enhanced electrical conductivity, improved cyclic stability, and superior electrochemical performance, making them practical for energy storage applications (Jacobsen *et al.*, 2020).

The electrochemical properties of Ce-MOF composites are typically evaluated using cyclic voltammetry (CV) and galvanostatic charge-discharge (GCD) techniques. These analyses consistently demonstrate the excellent specific capacitance and energy density of Ce-MOFs, which are attributed to their redox-active sites and porous structures (Zeng *et al.*, 2016). For instance, Ce-MOF/CeO_2 composites exhibit superior electrochemical performance compared to pristine Ce-MOFs, as the inclusion of CeO_2 enhances electrode stability and faradaic activity. Likewise, Ce-MOF/graphene and Ce-MOF/CNT composites show improved rate capability and capacitance retention, benefiting from the synergistic interaction between the MOF and the conductive additives (Yuan *et al.*, 2023).

Synthesis method for the formation of Ce-MOF

The Ce-MOF sample was synthesized using a hydrothermal method as described in (Yuan *et al.*, 2023). In this procedure, cerium nitrate hexahydrate ($Ce(NO_3)_3 \cdot 6H_2O$), and 2,6-naphthalene dicarboxylic acid were dissolved in deionized water and subjected to ultrasonic treatment for 30 minutes. The resulting solution was then transferred to a 100 mL Teflon-lined stainless-steel autoclave and heated at 60 °C for 20 hours. Afterward, the suspension was allowed to cool naturally to room temperature. The resulting precipitate was collected via centrifugation, washed thoroughly with deionized water, and dried at 60 °C for 24 hours.

4.5.1. Mechanism for the formation of Ce-MOF

Experimental findings have shown that during the synthesis of metal-organic frameworks (MOFs), an etching process simultaneously occurs, facilitating the incorporation of nanoparticles (NPs) into the MOF structure. This etching/immobilization approach results in a significant increase in oxygen vacancies, which are known to enhance the catalytic activity of the NPs. Specifically, during the synthesis of Ce-MOF, cerium nanoparticles (CeNPs) are introduced into the solution along with the ligand (Yang *et al.*, 2017).

The inclusion of CeNPs triggers surface etching, reducing the particle size and increasing the concentration of Ce^{3+} ions, thereby generating additional oxygen vacancies. This process ensures that the NPs are highly dispersed and stabilized within the MOF framework. The unique etching/immobilization strategy is expected to substantially improve the catalytic activity of Ce-MOF by leveraging the ultrasmall size of the NPs, the abundance of oxygen vacancies, and the elevated concentration of Ce^{3+} ions. Compared to colloidal CeNPs, this method provides superior dispersion and stability of the NPs within the MOF structure, which further enhances both the catalytic properties and electrochemical performance of the material (Babu *et al.*, 2009).

4.5.2. Preparation of Ce-MOF electrode

The Ce-MOF electrode was prepared by mechanically grinding a mixture of carbon black, Ce-MOF, and silicone oil. The resulting paste was then transferred into polymer tubes fitted with copper wire connections and left to dry at room temperature. Once dried, the electrode surface was smoothened using blotter paper, yielding the desired electrode ready for subsequent electrochemical testing.

4.6. Ce-MOF derived composites: Boost supercapacitor's efficiency

While MOFs hold great potential as materials for supercapacitor electrodes, they also face certain limitations, including poor electrical conductivity and particle aggregation. These issues can reduce porosity and lead to the degradation of electrode materials during charge-discharge cycles (Li *et al.*, 2021). However, MOF-based composites overcome these challenges by offering a synergistic combination of properties, introducing novel physical and chemical characteristics that outperform their individual components.

Composites derived from MOFs exhibit exceptional electronic conductivity, a large surface area, and substantial pore volume, making them highly effective for charge storage in supercapacitors (Mohanty *et al.*, 2021). These advantages position MOF composites as promising candidates for next-generation energy storage systems.

4.6.1. Ce-MOF/CeO_2

Cerium oxide exhibits a wide array of exceptional properties, making it a highly versatile material for diverse industrial applications. Its key attributes include excellent mechanical strength, multiple oxidation states, high light transmission, superior electrical conductivity, a large surface area, substantial oxygen storage capacity, numerous redox-active sites, and the presence of oxygen vacancies (Xie *et al.*, 2017). These unique characteristics make cerium oxide particularly valuable for electrochemical applications.

Notably, cerium oxide can undergo a reversible transformation between CeO_2, and CeO_{2-x} during redox processes, a behavior attributed to the creation of oxygen deficiencies and lattice defects within the cerium structure. This reversible transformation significantly enhances its utility in energy storage and catalytic systems.

The crystal structure of cerium oxide (ceria), depicted in Fig. 9, comprises a face-centered cubic fluorite lattice with a unit cell composition of Ce_4O_8.

 https://doi.org/10.37819/nanofab.9.2032

In this structure, each cerium atom is coordinated with eight oxygen atoms, while each oxygen atom is connected to four cerium atoms. With a molar mass of 140.12 g mol^{-1}, the estimated density of ceria is approximately 6.770 g cm^{-3} (Kowsuki *et al.*, 2023). At the nanoscale, the cubic fluorite structure of cerium oxide (CeO_2) remains stable, even with the presence of oxygen vacancies that serve as redox reaction sites. This structure includes three distinct low-index planes: (100), (110), and (111). Each plane exhibits unique characteristics, such as the presence or absence of dipole moments parallel to the surface, which can result in charged planes, neutralized planes, or surfaces without dipole moments. These surface properties and plane characteristics of cerium nanoparticles significantly influence molecular interactions and adsorption behavior on the cerium surface (Walkey *et al.*, 2015).

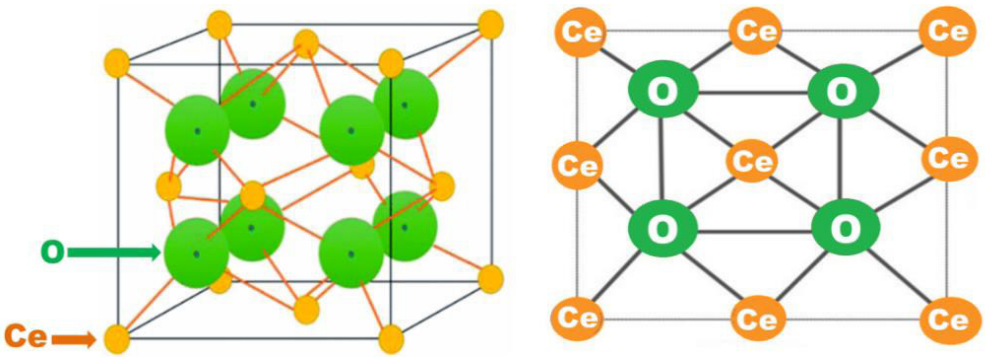

Figure 9. (a) Represents Ce4O8's fundamental fcc fluorite lattice in 3D (Mishra *et al.*, 2021), and (b) represents 2D project of the crystal structure. Adapted from Mishra *et al.*, Materials Today Comm., 28 (2021) 102562. Copyright 2021 Elsevier.

Ceria nanoparticles exhibit diverse morphologies, including rod-like shapes, octahedra, and cubes. Ceria-octahedra and ceria-cubes are well-faceted, with the former enclosing {111} facets and the latter enclosing {100} facets. In contrast, ceria-rods are less well-faceted, featuring complex exposed planes characterized by rough surfaces, numerous corners, and edges. This morphology includes both {111} and {100} facets, resulting in a spectrum that represents a superposition of the other two morphologies, as illustrated in Fig. 10 (Cao *et al.*, 2018).

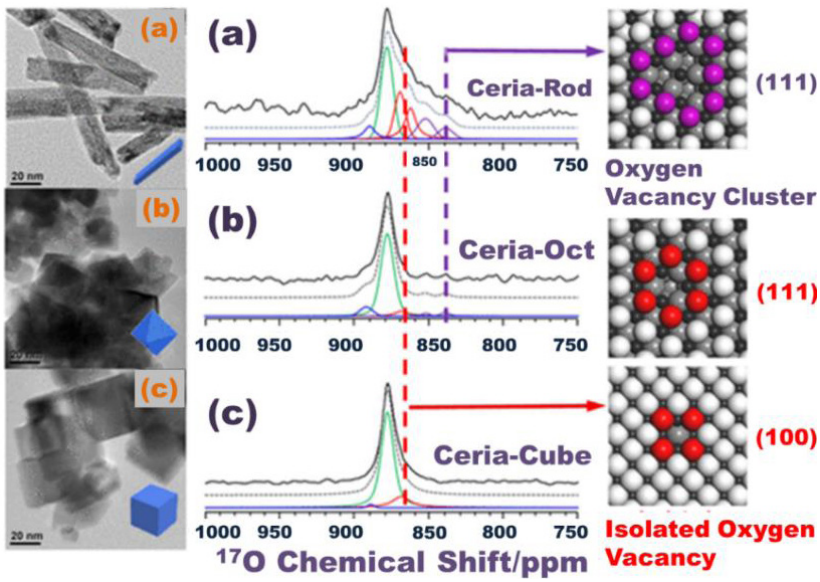

Figure 10. Relation between planes of Ceria and morphology (Cao *et al.*, 2018). Adapted from Cao *et al.*, J. Phys. Chem. C, 122 (2018) 35. Copyright 2018 ACS Publications.

Nallappan *et al.* investigated the electrochemical behavior of CeO_2 electrodes using cyclic voltammetry at various sweep rates and with different electrolytes, such as sodium chloride, potassium chloride, sodium sulfate, and potassium sulfate. The resulting curves, shown in Fig. 11, highlight the pseudocapacitive nature of CeO_2. The study revealed that as the size of the electrolyte ion increases, the diffusion rate decreases, leading to a reduction in capacitance (Maheswari *et al.*, 2015). These findings suggest that the pseudocapacitive performance of ceria is influenced by the size of ceria particles and the presence of structural defects.

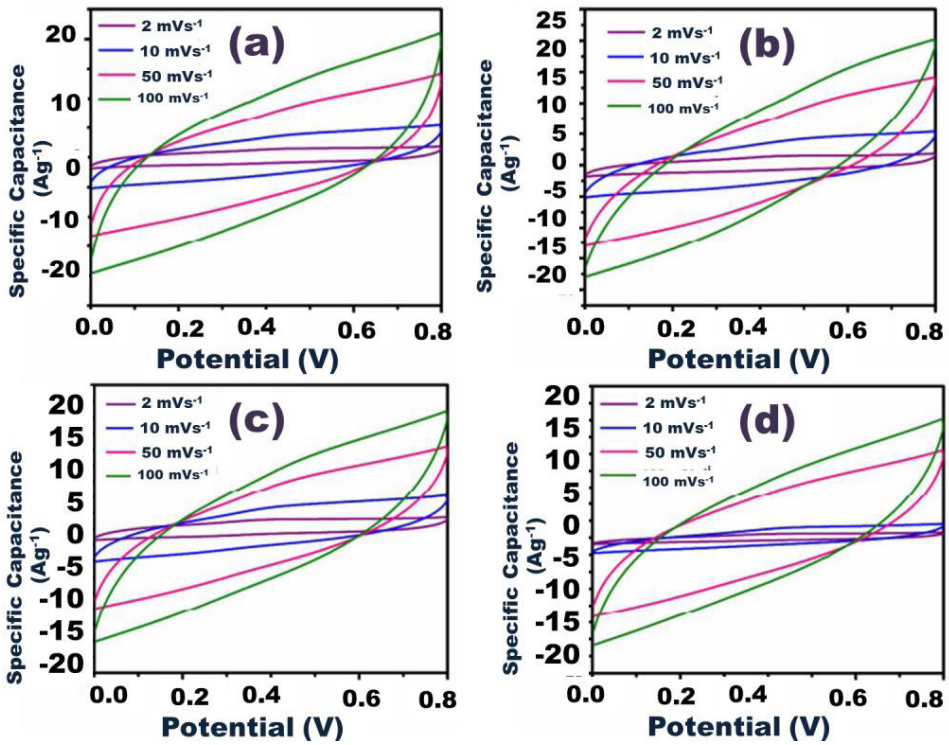

Figure 11. Cyclic voltammetry curves of CeO_2 nanoparticles which are obtained by using different electrolytes (a) NaCl (b) KCl, (c) Na_2SO_4, and (d) K_2SO_4 (Maheswari *et al.,* 2015). Adapted from Maheswari *et al.,* Energy & Fuels, 29 (2015) 12. Copyright 2015 ACS Publications.

The charge storage in this occurs through two mechanisms: (i) the absorption and desorption of M^+ ions on the surfaces, and (ii) the intercalation and de-intercalation of M^+ ions on the surface.

Material used	Size of particle	Method of synthesis	Application
Zr doped CeO_2	10-20 nm	Force hydrolysis sintering	Polymer electrolyte membrane additive
Nano CeO_2-Polymer composite	< 25nm	Commercial	Polymer ceramic composite Li-ion battery separator
Nano CeO_2 loaded carbon	3-5 nm	Thermal hydrolysis	Li-S battery cathode
Co-doped CeO_2	4-7 nm	Hydrothermal	ORR/Supercapacitor
Pd/C-CeO_2	20-40 nm	Thermal hydrolysis	Anode catalyst for pt free anion exchange membrane fuel cells
Ni doped CeO_2	Grain size	Microwave-assisted sol-gel	Supercapacitor

Table 2. Applications of cerium oxide in energy storage (Wang *et al.,* 2020).

 https://doi.org/10.37819/nanofab.9.2032

The chemical equation representing the non-faradaic process is as follows:

$$(CeO_2)_{surface} + M^+ + e^- \rightleftharpoons (CeO_2.M^+)_{surface} \quad (7)$$

The chemical equation representing the faradaic process is as follows:

$$CeO_2 + M^+ + e^- \rightleftharpoons CeOOM \quad (8)$$

where $M^+ = Na^+, K^+$.

The morphology and crystal planes of CeO_2 nanostructures play a critical role in their electrochemical charge storage capabilities. Controlling the morphology of CeO_2 nanostructures promotes the formation of highly reactive crystal planes, enhancing the electrochemical charge storage and rate performance of energy storage devices (Jeyaranjan *et al.*, 2020). Oxygen vacancies on specific crystal planes correlate directly with their redox-type storage capacity, making the morphology of ceria nanoparticles a key determinant of pseudocapacitance. Different ceria nanoparticle morphologies contribute uniquely to supercapacitor performance. For example, 0D cerium oxide nanoparticles exhibit a capacitance of 134.6 Fg^{-1} at 1 Ag^{-1}, while 0D hexagonal-shaped cerium oxide nanostructures achieve a capacitance of 927 Fg^{-1} at 2 A g^{-1}. Similarly, 1D dumbbell-shaped cerium oxide nanoparticles demonstrate a capacitance of 779 Fg^{-1} at 1 A g^{-1}, whereas 1D cerium oxide nanorods exhibit a capacitance of 162.47 Fg^{-1} at 1 A g^{-1} (Ponnaiah *et al.*, 2021).

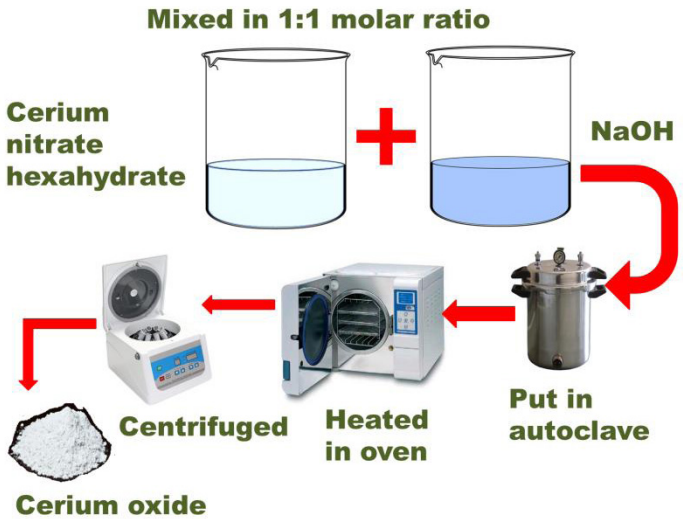

Figure 12. Process of synthesis of ceria by hydrothermal method.

Ceria nanoparticles can be synthesized using cost-effective methods such as the sol-gel method, co-precipitation method, and hydrothermal method. These techniques enable the production of ceria nanoparticles with tailored morphologies, which can be further doped with other substances to enhance their functional properties. A summary of these methods and applications is provided in Table 3. Cerium oxide's abundance, cost-effectiveness, and high porous surface area make it a promising material for supercapacitors. Its inclusion in energy storage systems improves capacity, lowers input resistance, enhances cycle stability, and boosts charge-discharge efficiency, making it an attractive option for next-generation energy storage technologies (Gong *et al.*, 2018).

The electrochemical properties of cerium oxide nanoparticles synthesized via the hydrothermal technique are commonly evaluated using galvanostatic methods. Beyond its redox activity, ceria exhibits free radical scavenging capabilities, further broadening its application potential. The hydrothermal synthesis process for cerium oxide is illustrated in Fig. 12. The procedure involves mixing hydrated cerium nitrate with deionized water and sodium hydroxide, followed by stirring the solution at room temperature. This mixture is then transferred to an autoclave and heated in an oven at 200 °C. The resulting precipitates undergo multiple centrifugation steps using deionized water and ethanol. Finally, the product is dried in an oven at 60 °C to yield the desired cerium oxide nanoparticles (Pujar *et al.*, 2020).

CeO_2-based materials have been widely studied for their potential applications in lithium-ion batteries, serving as both anode and cathode materials. As an anode material, CeO_2 offers a high theoretical capacity and excellent cycling stability. However, its electrochemical performance is hindered by poor electronic conductivity, which limits its practical application (Liu *et al.*, 2016). In the context of supercapacitors, CeO_2-based materials have gained attention for their high power density and rapid charge-discharge capabilities. The high surface area and redox-active properties of CeO_2 contribute to its pseudocapacitance behavior, enabling enhanced energy storage performance. To address its limitations, hybrid materials combining CeO_2 with carbon nanomaterials have been developed. These composites exhibit improved specific capacitance and enhanced cycling stability, overcoming the inherent conductivity issues of pure CeO_2. CeO_2-based supercapacitors hold significant promise for applications requiring rapid energy storage and delivery, such as electric vehicles and portable electronic devices, offering a viable pathway for next-generation energy storage technologies (Ghosh *et al.*, 2020).

4.6.2. Synthesis of CeO_2 contact interface with Ce-MOF

To enhance the activity of cerium oxide, significant efforts have been made, including structural modifications such as the incorporation of defect sites, introduction of oxygen vacancies, and heteroatom doping. Despite these advancements, cerium oxide nanoparticles are prone to aggregation, which reduces their surface area and diminishes their catalytic and electrochemical activity. To address this limitation, nanoparticles are embedded into metal-organic frameworks (MOFs) within their porous hosts. MOFs stabilize the nanoparticles, prevent aggregation, and offer a larger accessible surface area. Additionally, the open channels of MOFs facilitate access to the active sites of cerium oxide, further enhancing its activity (Yang *et al.*, 2017).

CeO_2-MOF composites combine the high surface area, tunable porosity, and redox properties of MOFs with the catalytic and electrochemical properties of CeO_2, yielding highly stable and efficient materials for supercapacitor applications. The synergistic interaction between CeO_2, and MOFs amplifies their individual properties, resulting in superior overall performance.

Synthesis of CeO2 -MOF Composites

The synthesis of CeO_2-MOF composites involves combining CeO_2 precursors with MOF components in a suitable solvent under controlled conditions. One common approach is solvothermal synthesis, where CeO_2 nanoparticles and MOF precursors are mixed and subjected to controlled heating. For instance, cerium nanoparticles are mixed with a solvent such as dimethylformamide (DMF) in one vial, while benzenedicarboxylic acid is dissolved in DMF in another. These solutions are combined and placed in an oil bath at 100°C. Ammonium cerium nitrate is then added to the mixture while stirring for 30 minutes. The resulting precipitate is washed, dried, and activated under vacuum to obtain the CeO_2-MOF composite (Fig. 13) (Lammert *et al.*, 2015).

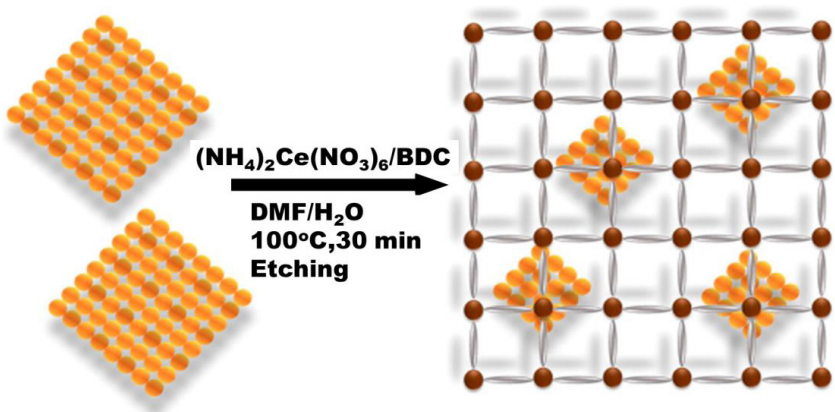

Figure 13. Typical diagram representing the immobilization of cerium nanoparticles in the MOFs (Hassan *et al.*, 2020). Adapted from Hassan *et al.*, ACS Appl. Nano Mater., 3 (2020) 4. Copyright 2020 ACS Publications.

Another method for synthesizing CeO_2-MOF composites is the co-precipitation technique. This approach involves the simultaneous precipitation of CeO_2 and MOF components from a common precursor solution. By adjusting reaction parameters such as temperature, pH, and the ratio of CeO_2 to MOF components, the formation of well-integrated CeO_2-MOF composites can be controlled. For example, a solution of 1,3,5-tricarboxylic acid in ethanol is mixed with cerium nitrate hexahydrate in ethanol and stirred briefly. The mixture is left undisturbed overnight, and the resulting precipitate is washed and dried to yield the final product (Ramachandran *et al.,* 2018).

4.7. Ce-MOF/GO

Graphene, with its two-dimensional (2D) crystalline structure, possesses extraordinary electronic, optical, and mechanical properties. Within its crystal lattice, graphene's charge carriers, electrons, exhibit ballistic movement, which enables remarkably high electrical conductivity, despite its organic nature (Brownson *et al.,* 2013). Composed entirely of sp^2-hybridized carbon atoms, graphene offers a suite of exceptional characteristics, including high electrical and thermal conductivity, lightweight, chemical stability, excellent mechanical strength, and a tunable surface area of up to 2675 $m^2 g^{-1}$ (Xia *et al.,* 2009). These properties make graphene and graphene-based materials indispensable for applications in high-performance structural nanocomposites, electronics, environmental protection, and energy devices, including energy generation and storage (Liang *et al.,* 2011). Such applications span technologies like Li-ion batteries, fuel cells, supercapacitors, photovoltaic systems, and solar cells. Notably, single-layer graphene exhibits a theoretical specific capacitance of approximately 21 µF cm 2, which corresponds to a specific capacitance of roughly 550 F g^{-1} when its entire surface area is utilized (Xia *et al.,* 2009).

Extensive research has focused on graphene-based materials as conductive frameworks to facilitate redox reactions in transition metal oxides, hydroxides, and conducting polymers. Nano-hybrid electrodes comprising graphene and nanoparticles of transition metal oxides, hydroxides, or conductive polymers demonstrate remarkable electrochemical performance. This performance arises from synergistic effects, where graphene layers improve nanoparticle dispersion, serve as highly conductive matrices to enhance electrical conductivity, and provide structural support, while metal oxides, hydroxides, or conducting polymers contribute significant pseudocapacitance.

Graphene is essentially a monolayer of graphite, while graphene oxide (GO) is a key derivative of graphene. GO, which can be readily synthesized from graphite, retains a layered structure and exhibits surface-related properties. Depending on the synthesis method, GO may possess various surface functional groups distributed differently across its structure. Oxygen-containing functional groups such as hydroxyl, carboxyl, and epoxy groups are typically located around the edges of graphene sheets, aiding in the stabilization of quasi-2D sheets. On the basal plane, GO typically features phenol epoxy and epoxide groups, while ionizable carboxylic acid groups are situated at the sheet edges (Cai *et al.,* 2011).

Graphene can be organized into diverse structural forms, including free-standing particles or dots, one-dimensional fibers or yarns, two-dimensional films, and three-dimensional foams or composites. While mechanical exfoliation is capable of producing high-quality graphene, this method is limited in scalability and is mainly suitable for research purposes. As an alternative, chemical oxidation processes can produce graphene oxide (GO) on a larger scale. Reduced graphene oxide (rGO), derived from GO, serves as a foundational material for energy storage devices due to its enhanced conductivity and structural versatility (Liu *et al.,* 2021).

4.7.1. Synthesis of Ce-MOF derived GO composite

The incorporation of graphene oxide (GO) into Ce-MOF significantly enhances its specific capacitance and energy density, which has been measured at approximately 233.8 F g^{-1} in 3 M KOH solution (Ramachandran *et al.,* 2018). This improvement is primarily attributed to the pseudocapacitance contribution of oxygen-containing functional groups present in GO.

To synthesize Ce-MOF-based GO composites, H_3BTC (1,3,5-benzenetricarboxylic acid) is first dissolved in a 3:1 mixture of water and ethanol (by volume). A small quantity of graphene oxide is then added to this solution and sonicated for a specific duration to ensure proper dispersion. The resulting solution is left undisturbed in a beaker overnight to allow stabilization. The precipitate is subsequently

washed with ethanol and dried to yield the desired Ce-MOF/GO composite (Ramachandran *et al.*, 2018).

4.8. Ce-MOF/CNT

Carbon nanotubes (CNTs) have garnered significant attention for their exceptional structural, electrical, and mechanical properties, making them valuable materials for various technological applications. CNTs are formed when a graphite sheet is rolled into cylindrical shapes, resulting in single-walled CNTs (SWCNTs) and multi-walled CNTs (MWCNTs). They exhibit a unique structural design, nanometer-scale dimensions, high surface area, low electrical resistivity, and remarkable stability, all of which make them excellent candidates for use in polarizable electrodes. Both SWCNTs and MWCNTs have been extensively studied for their application in electrochemical supercapacitor electrodes, leveraging these properties (Venkataraman *et al.*, 2019).

CNTs possess several remarkable attributes, including cost-effectiveness, lightweight nature, high aspect ratios, expansive surface area, superior optical characteristics, exceptional thermal and electrical conductivity, and outstanding mechanical strength. These characteristics make CNTs highly versatile for a variety of applications in electronics, biomedicine, and industrial sectors. For instance, CNTs hold significant potential in advancing electronics "beyond CMOS," serving as active devices and interconnects in future integrated circuits (Agarwal *et al.*, 2018).

CNTs belong to the fullerene family, a group of carbon allotropes with cage-like structures, including hollow spheres, ellipsoids, and cylindrical tubes. Fullerenes are composed of interconnected graphene sheets with hexagonal and pentagonal rings, forming their distinctive curved architecture. The carbon atoms in CNTs are sp^2-hybridized, which are mechanically stronger compared to sp^3-hybridized carbons in diamond, resulting in exceptional strength and stiffness. Theoretical calculations estimate the specific surface area (SSA) of an individual SWCNT to be approximately 1315 m^2/g. However, actual measured SSAs are often lower due to bundling, agglomeration, and impurities in the tubes. For MWCNTs, the SSA primarily depends on the number of walls, with measured values ranging from 680-850 m^2/g for two-walled CNTs to around 500 m^2/g for three-walled CNTs (Peigney *et al.*, 2001).

CNTs also possess excellent thermal properties and intriguing dimensional characteristics, including a high aspect ratio. Their exceptional charge carrier mobility makes them highly promising for various electronic applications. Notably, the bandgap of semiconducting CNTs exhibits an inverse relationship with their diameter, calculated using the formula:

$$E_{gap} = \frac{2\gamma_0 a_{c\text{-}c}}{d} \quad (9)$$

where γ_0, represents the C–C tight-binding overlap energy (2.45 eV), a_{c-c} is the nearest-neighbor C–C bond distance (0.142 nm), and d is the diameter of the CNT (Matsuda *et al.*, 2010).

These exceptional properties position CNTs as critical materials for a wide range of emerging technologies in energy storage, electronics, and beyond.

4.8.1. Synthesis of Ce-MOF derived CNT composite

To enhance the specific capacitance of Ce-MOF, it is combined with carbon nanotubes (CNTs). The integration of MOFs with CNTs improves the conductivity of energy storage devices by increasing the surface area and providing greater cyclic stability (Anwer *et al.*, 2023). For example, Ramachandran *et al.* reported a specific capacitance of 94.8 F g^{-1} for Ce-MOF and 129.6 F g^{-1} for Ce-MOF/CNT composites in KOH electrolyte at a current density of 1 A g^{-1} (Ramachandran *et al.*, 2018).

The synthesis of Ce-MOF/CNT composites involves dissolving H_3BTC (1,3,5-benzenetricarboxylic acid) in a 3:1 mixture of water and ethanol by volume. A small quantity of carbon nanotubes is then added to this solution, which is sonicated to ensure proper dispersion. The mixture is left undisturbed overnight in a beaker to stabilize. The resulting precipitate is washed with ethanol and dried to obtain the desired Ce-MOF/CNT composite (Ramachandran *et al.*, 2018).

4.8.2. Characterization techniques for Ce-MOF composites

XRD characterization

X-ray diffraction (XRD) analysis is a widely used technique for determining the crystalline structure of Ce-MOF composites. The diffraction patterns

 https://doi.org/10.37819/nanofab.9.2032

provide crucial insights into the crystal phases present, the degree of crystallinity, and any phase changes or interactions between Ce-MOF and other components. Additionally, XRD can be used to evaluate stress and strain within the crystal lattice. Ce-MOF exhibits a fine structure with a high degree of crystallinity, evidenced by the sharpness and clarity of its diffraction peaks. The powder XRD (PXRD) pattern of Ce-MOF aligns with a distinct group of lanthanide-based MOFs (Ln-BTC). In these structures, each BTC linker coordinates with six Ce^{3+} ions, and each carboxylate group of the linker forms bonds with two different Ce^{3+} ions.

The inorganic building block of Ce-MOF consists of distorted pentagonal CeO_7-bipyramids, where six oxygen atoms belong to carboxylate groups, and one oxygen atom is associated with a solvent molecule, such as water or DMF. These CeO_7 units oscillate in two directions within the plane, assembling into helical chains that create 43-screw axes, ultimately forming square-shaped, non-interconnected channels (Ethiraj *et al.*, 2016).

Ramachandran *et al.* investigated the XRD pattern of Ce-MOF doped with GO and CNT, concluding that the crystallinity of Ce-MOF is retained even after doping, as shown in Fig. 14(a) (Ramachandran *et al.*, 2018). The XRD pattern of Ce-MOF reveals peaks at 2θ angles of 7.2°, 8.3°, 11.7°, 13.8°, and 14.4°, corresponding to the crystal planes (111), (200), (220), (311), and (222), respectively (Hassan *et al.*, 2020).

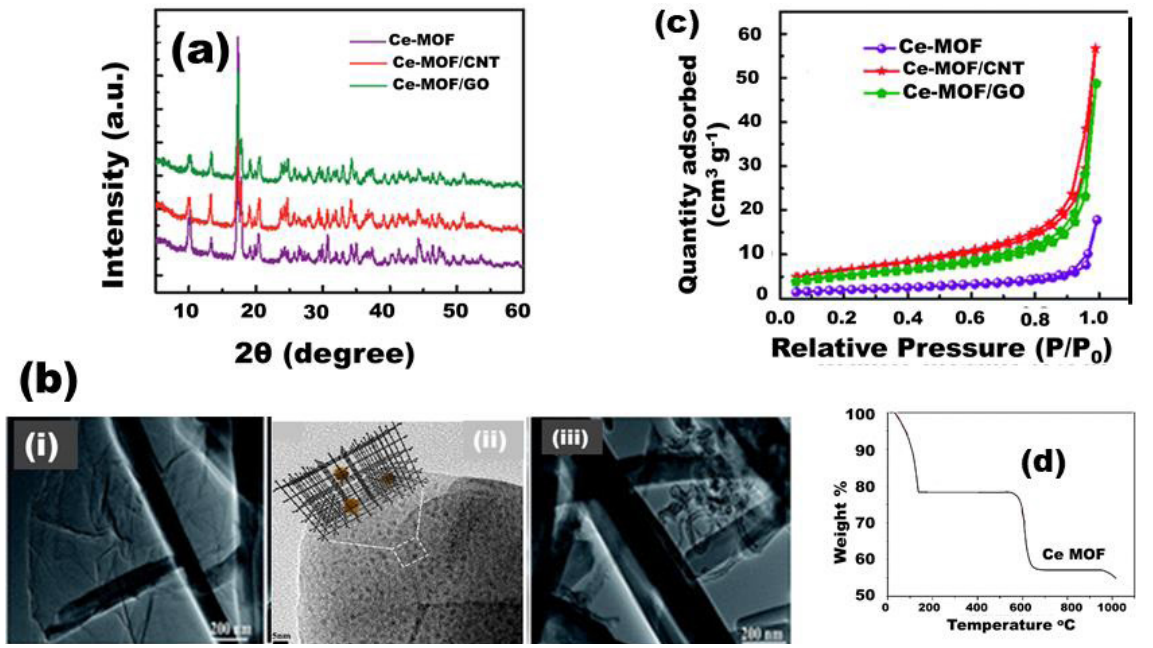

Figure 14. (a) X-ray diffraction pattern of Ce-MOF (Ramachandran *et al.,* 2018). Adapted with permission under an CC BY-NC 3.0 from Ramachandran *et al.,* RSC advances, 8, 7 (2018). Copyright 2018 Royal Society of Chemistry; (b) TEM image of (i) Ce- MOF/GO (Ramachandran *et al.,* 2018); (ii) Ce-MOF/CeO_2 (Hassan *et al.,* 2020); (iii) Ce-MOF/CNT (Ramachandran *et al.,* 2018). Adapted from Hassan *et al.,* ACS Appl. Nano Mater., 3, 4(2020). Copyright 2020 ACS Publications; Adapted with permission under an CC BY-NC 3.0 from Ramachandran *et al.,* RSC advances, 8,7(2018). Copyright 2018 Royal Society of Chemistry, (c) BET measurement for determining the surface area (Ramachandran *et al.,* 2018), Adapted with permission under an CC BY-NC 3.0 from Ramachandran *et al.,* RSC advances, 8,7(2018). Copyright 2018 Royal Society of Chemistry; (d) TGA for determining the thermal stability of cerium oxide-MOF (Peng *et al.,* 2019). Adapted with permission under an CC BY-NC-ND 3.0 from Peng *et al.,* Arab. J. Chem.,12,7(2019). Copyright 2019 Elsevier.

Ahmed *et al.* analyzed the PXRD patterns of Ce-MOF, GO, and GO@Ce-MOF, observing similar peaks for Ce-MOF and GO@Ce-MOF at 2θ values of 8.5°, 17.3°, 20.5°, 24.7°, and 34.2°. However, no peak was observed at a 2θ value of 12°, which corresponds to the GO structure. This absence indicates

that the GO@Ce-MOF crystals are uniformly distributed within the spaces between GO sheets, suggesting that GO does not interfere with the synthesis of Ce-MOF. The resulting Ce-MOF composite exhibits well-organized Ce-MOF units within the structure. The diffraction peaks of GO@Ce-MOF confirm that the presence of GO does not hinder the crystallization of Ce-MOF or the formation of composites containing the Ce-MOF framework (Ahmed Malik *et al.,* 2022).

TEM analysis

Transmission electron microscopy (TEM) is a critical tool for analyzing the morphology, size, and dispersion of CeO_2, GO, and CNT nanoparticles within the MOF framework. TEM images provide detailed insights into the composite's structure, particle size distribution, and the interface between Ce-MOF and its composite components. Hassan *et al.* used TEM to examine Ce-MOF-derived ceria composites, as shown in Fig. 14(b)(ii), revealing that the immobilization and etching of cerium oxide within the Ce-MOF matrix result in reduced particle size. This size reduction and the uniform dispersion of cerium nanoparticles are attributed to the chemical etching process (Hassan *et al.,* 2020).

Similarly, Ramachandran *et al.* analyzed TEM images of Ce-MOF-derived GO and CNT composites, shown in Fig. 14(b)(i) and Fig. 14(b)(iii), respectively. The images depict wrinkled graphene oxide sheets uniformly decorated with Ce-MOF nanorods, highlighting how GO prevents aggregation of Ce-MOF (Ramachandran *et al.,* 2018). TEM images also show slight differences in morphology and structure for Ce-MOF/CNT and Ce-MOF/GO composites, which are linked to higher carbon content in the composites. Huang *et al.* further observed from TEM images that adding CNTs to Ce-MOF reduces the aggregation of Ce-MOF granules and improves the dispersion of Ce-MOF nanocomposites within CNT matrices (Huang *et al.,* 2021).

FTIR Analysis

Fourier transform infrared (FTIR) spectroscopy is employed to identify chemical bonds and functional groups in Ce-MOF composites. FTIR spectra provide insights into interactions between cerium and MOF components, such as coordination bonds or hydrogen bonding. A band at 3393 cm^{-1} indicates the presence of OH^{-1} groups and adsorbed water molecules, while asymmetric and symmetric vibrations of carboxylate ions are observed at 1611-1555 cm^{-1} and 1434-1370 cm^{-1}, respectively, confirming the presence of carboxylate ions within the MOF structure. These vibrations occur at lower wavenumbers than those of typical C=O stretching bands (1690-1760 cm^{-1}, suggesting deprotonation of carboxylic acids into carboxylate groups. The Ce-O stretching vibration appears as a band at 533 cm^{-1} (Maiti *et al.,* 2014).

Ahmed *et al.* analyzed the FTIR spectra of BTC linkers, Ce-MOF, GO, and GO@Ce-MOF. They observed carboxylic acid stretching vibrations in the spectra but noted the disappearance of strong carbonyl absorption bands at 1693 cm^{-1}, indicating the full deprotonation of carboxylic acids into carboxylates in Ce-MOF (Ahmed Malik *et al.,* 2022). Additionally, aromatic C=C vibrations were detected at 1563, 1558, and 1525 cm^{-1}. For GO, major stretching vibrations were observed at 3433 and 3394 cm^{-1} (O-H), 2929 and 2857 cm^{-1} (CH_3/CH_2, 1723 cm^{-1} (C=O in carbonyl/carboxyl groups), 1628 cm^{-1} (C=C), and 1050 cm^{-1} (C-O-C). These bands confirm the presence of oxygen functional groups (Yang *et al.,* 2020).

Huang *et al.* noted a similar FTIR pattern for GO@Ce-MOF compared to Ce-MOF, with no oxygen-containing GO groups visible, suggesting successful grafting of Ce-MOF onto the GO surface. For Ce-MOF/CNT composites, Shen *et al.* reported FTIR spectra similar to Ce-MOF, with no detectable carboxylic stretching bands for CNT, as carboxylic groups on the CNT surface were consumed during Ce-MOF crystal growth (Cao *et al.,* 2015; Shen *et al.,* 2021).

BET Analysis

Brunauer-Emmett-Teller (BET) analysis provides crucial information on the specific surface area and pore characteristics of Ce-MOF composites, which are vital for applications like gas adsorption, catalysis, and energy storage. BET analysis measures nitrogen adsorption-desorption isotherms to estimate surface area, with results expressed in square meters per gram (m^2/g). The Ce-MOF composite sample is subjected to stepwise adsorption of nitrogen gas at varying pressures, generating a BET isotherm that relates gas adsorption to relative pressure. This analysis provides insights into the surface area, pore size distribution, and multilayer adsorption behavior of the material.

 https://doi.org/10.37819/nanofab.9.2032

According to Ramachandran *et al.*, as illustrated in Fig. 14(c), the specific surface area was measured to be 7.10 m^2/g for Ce-MOF, 22.86 m^2/g for Ce-MOF/CNT, and 18.83 m^2/g for Ce-MOF/GO. The pore size distribution centered at 3.8 nm for Ce-MOF indicates the presence of mesopores in the material (Ramachandran *et al.*, 2018). These findings highlight the role of composites in improving the surface area and pore structure, enhancing their suitability for energy storage applications.

TGA analysis

Thermogravimetric analysis (TGA) is a valuable technique for evaluating the thermal stability and decomposition behavior of Ce-MOF composites. TGA provides detailed information on the thermal stability of the composite and the weight loss associated with the decomposition of its organic components. The TGA curve for Ce-MOF typically shows mass loss occurring in three distinct steps, corresponding to different temperature ranges. The first step involves the loss of adsorbed or bound water molecules within the range of 80-150 °C. The second step, observed between 200-300 °C, corresponds to the decomposition of extra organic components within the composite. The final step, occurring between 320-420 °C, involves the breaking of coordination bonds between the ligand and the metal framework, leading to further decomposition.

Xiong *et al.* analyzed the TGA of Ce-MOF composites and provided the corresponding TGA curve, shown in Fig. 14(d), which illustrates these decomposition steps and highlights the thermal stability of Ce-MOF across various stages.

4.8.3. Electrochemical properties of Ce-MOF-derived composites

The electrochemical properties of Ce-MOF and its composites have garnered significant attention for their potential in high-performance energy storage devices like supercapacitors. The composites of Ce-MOF exhibit high specific capacitance, a critical parameter determining the amount of charge stored per unit mass or volume of the material. Ce-MOF's high surface area and porosity provide abundant active sites for charge storage, facilitating efficient ion adsorption and desorption during charge-discharge cycles. By optimizing the composition, morphology, and porosity of Ce-MOF, its specific capacitance can be significantly enhanced (Zeng *et al.*, 2016).

Ce-MOF exhibits pseudocapacitive behavior, primarily due to reversible redox reactions at the electrode-electrolyte interface. The presence of redox-active species, such as Ce^{3+}/Ce^{4+} couples within the Ce-MOF structure, contributes to faradaic charge storage, complementing the electrostatic double-layer capacitance. This pseudocapacitive behavior results in higher capacitance and improved energy storage performance in supercapacitors (Maiti *et al.*, 2014). Furthermore, Ce-MOF composites demonstrate excellent cycling stability, ensuring long-term reliability in supercapacitor applications. The robust MOF framework, combined with the stable redox activity of CeO_2, GO, and CNT, preserves the structural integrity of the material during repeated charge-discharge cycles.

Electrochemical Studies

To evaluate the energy storage potential of Ce-MOF composites, various electrochemical techniques are employed, including cyclic voltammetry (CV), galvanostatic charge-discharge (GCD), and electrochemical impedance spectroscopy (EIS). These methods provide critical insights into the capacitance, charge-discharge dynamics, and cycling stability of Ce-MOF composites when used as electrode materials for batteries and supercapacitors.

Cyclic Voltammetry (CV) Studies

Cyclic voltammetry (CV) is a widely used technique for analyzing the electrochemical and redox behavior of Ce-MOF composites. This method involves applying a potential waveform to the electrode and recording the resulting current response, providing valuable data on redox reactions, capacitive behavior, and electrode stability.

Fatemi *et al.* conducted CV measurements of Ce-MOF electrodes at various scan rates using a three-electrode setup, as shown in Fig. 15(a). The results demonstrated that the redox rate increases proportionally with the square root of the scan rate, indicating that the electrochemical processes are diffusion-controlled (Sangeetha *et al.*, 2020). Moreover, the CV plot deviates from an ideal rectangular shape due to the pseudocapacitive behavior of Ce-MOF. The observed redox peaks in the CV plot correspond to faradaic reactions occurring on the electrode surface, involving changes in the oxidation states of cerium (Fatemi *et al.*, 2022).

$$Ce(III) + OH^- \rightleftharpoons Ce(III)(OH)^-_{ad} \quad (9)$$

$$Ce(III)(OH)^-_{ad} \rightleftharpoons Ce(IV)(OH)_{ad} + e^{-1} \quad (10)$$

The incorporation of graphene oxide (GO) into Ce-MOF composites significantly enhances the cycling stability of Ce-MOF (Ahmed Malik *et al.*, 2022). Shen *et al.* reported that the cyclic voltammetry (CV) curves of CNTs exhibit a rectangular shape with no distinct peaks, reflecting their electrochemical double-layer behavior. In contrast, the CV curves of Ce-MOF and Ce-MOF/CNT nanocomposites display broad redox responses, with anodic and cathodic peaks observed around +0.7 V and +0.4 V, respectively. These peaks correspond to the reversible electrochemical reaction of Ce^{4+}/Ce^{3+} redox couples in the nanocrystals (Shen *et al.*, 2021).

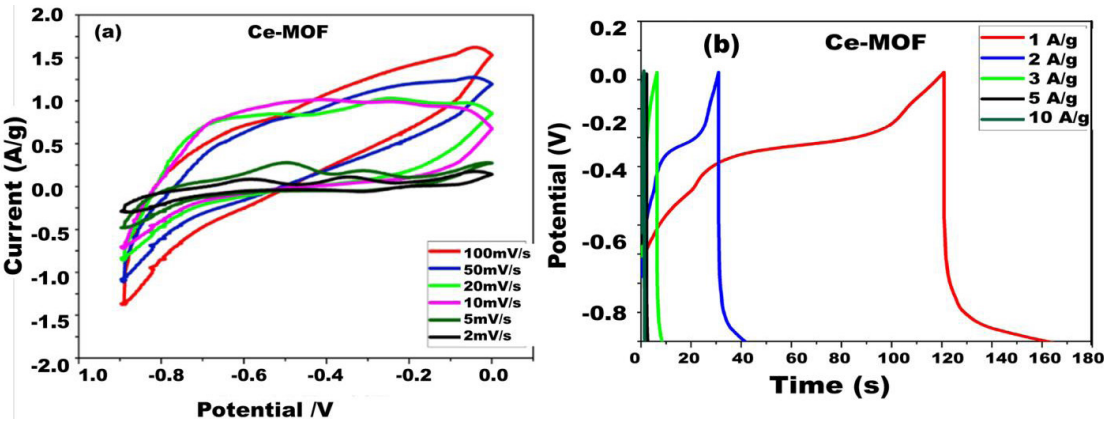

Figure 15. (a) Ce-MOF electrode's CVs obtained at the different scan rates; (b) GCD curves of Ce-MOF (Fatemi *et al.*, 2022). Adapted from Fatemi *et al.*, J. Energy Storage, 55 (2022) 105545. Copyright 2022 Elsevier.

Interestingly, redox peaks expected in the potential range more positive than +0.7 V are absent in Ce-MOF/CNT composites. This absence is attributed to the electrochemical reaction of cerium edge sites in the MOF crystals that are coordinated to the CNT surface. Additionally, Ce-MOF/CNT nanocomposites exhibit broader and overlapping redox peaks with larger enclosed areas in their CV curves compared to pristine CNTs, indicating a significant increase in pseudocapacitance.

As the scan rate increases, the specific capacitance of the material decreases. This behavior is due to reduced diffusion of electrolyte ions into the electrode structure at higher scan rates, which limits ion storage capacity.

Galvanostatic Charge-Discharge (GCD)

Galvanostatic charge-discharge (GCD) testing is performed by applying a constant current to the Ce-MOF electrode for a set period, followed by discharging the stored charge at the same current density. GCD measurements provide key information on specific capacitance, energy density, power density, supercapacitive behavior, and cycling stability of Ce-MOF-based composite materials.

As shown in Fig. 15(b), the GCD analysis of Ce-MOF exhibits nonlinear and asymmetrical charge-discharge curves. This behavior is attributed to the pseudocapacitive nature and partial irreversibility of charge storage mechanisms in Ce-MOF (Fatemi *et al.*, 2022). The specific capacitance of the electrodes can be calculated using the following equation:

$$C_{sp} = \frac{I \cdot \Delta t}{m \cdot \Delta V}$$

where:

- C_{sp} is the specific capacitance (F g^{-1}),
- I is the discharge current (A),
- Δt is the discharge time (s),
- m is the mass of the active material (g),
- ΔV is the potential window during discharge (V).

The GCD technique highlights the superior charge-discharge characteristics of Ce-MOF and its composites, further validating their potential in energy storage applications.

$$SC = \frac{It_d}{m(V_c - V_a)} \quad (11)$$

 https://doi.org/10.37819/nanofab.9.2032

In the equation used to calculate specific capacitance, I represents the charge-discharge current (A), tdt d is the discharge time (s), m is the mass of the active material (g), and $(V_c - V_a)$ denotes the potential window (V).

The galvanostatic charge-discharge (GCD) curves of Ce-MOF and its composites (Ce-MOF/CNT and Ce-MOF/GO) at different current densities in 3M KOH and 3M KOH + $K_3Fe(CN)_6$ electrolytes exhibit non-triangular shapes, indicative of pseudocapacitive behavior. These curves display plateaus at a potential of 0.2 V, corresponding to the faradic redox reaction of Ce^{2+}/Ce^{3+} with OH^-. The addition of the redox additive $K_3Fe(CN)_6$ to the KOH electrolyte shifts the plateau potential to 0.18 V, reflecting the redox reaction of $K_3Fe(CN)_6$. The maximum specific capacitance values for Ce-MOF, Ce-MOF/CNT, and Ce-MOF/GO are 94.8, 129.6, and 233.8 Fg^{-1}, respectively, at a current density of 1 A g^{-1}. These values increase further with the addition of $K_3Fe(CN)_6$ (Ramachandran *et al.*, 2018).

To evaluate the cyclic stability of the electrode materials, galvanostatic charge-discharge tests were performed. Ramachandran *et al.* conducted these tests at 3 A g^{-1} in KOH electrolyte and found that Ce-MOF/GO electrodes demonstrated higher capacitance retention compared to pure Ce-MOF and Ce-MOF/CNT electrodes, indicating superior rate capability and excellent electrochemical cyclic stability (Ramachandran *et al.*, 2018). Additionally, tests incorporating 0.2M $K_3Fe(CN)_6$ in 3M KOH electrolyte revealed improved cycle life and superior electrochemical stability compared to pure KOH electrolyte.

The Coulombic efficiency, which quantifies the charge retention and stability of electrode materials during charge-discharge processes, is a key metric for evaluating long-term performance. This metric highlights the effectiveness of Ce-MOF/GO composites, particularly in electrolytes enhanced with redox additives, for durable and reliable energy storage applications (Wang *et al.*, 2012).

$$\eta = \frac{t_d * 100}{t_c} \quad (12)$$

where t_d is the discharge time(s), t_c is the charging time(s).

The initial Coulombic efficiencies of Ce-MOF composites are relatively low, primarily due to the agglomeration of Ce-MOF nanorods and the restacking of GO and CNT layers. However, the Coulombic efficiencies improve significantly in 3M KOH+0.2M $K_3Fe(CN)_6$ electrolytes. This enhancement is attributed to the faradic redox reactions of $Fe(CN)_6/Fe(CN)_6$ occurring simultaneously with the Ce^{3+}/Ce^{2+} redox couple during the discharge process (Su *et al.*, 2009). These concurrent redox reactions result in a longer discharge time relative to the charging time, thereby increasing the Coulombic efficiency of the system.

Electrochemical Impedance Spectroscopy (EIS)

Electrochemical impedance spectroscopy (EIS) is a powerful technique used to evaluate the electrochemical behavior and performance of Ce-MOF composite electrodes. By examining the impedance response across a range of frequencies, EIS provides detailed insights into key parameters such as charge transfer resistance, ion diffusion, and electrode-electrolyte interface behavior. This technique is particularly useful for understanding the kinetic processes and interfacial properties of Ce-MOF electrodes.

Ion diffusion within the material can be analyzed from the low-frequency region of the Nyquist plot. The slope of this region reflects the resistance encountered by ions penetrating the electrode; a steeper slope indicates lower ion diffusion resistance (Fatemi *et al.*, 2022).

Ahmed *et al.* investigated the EIS performance of Ce-MOF and GO@Ce-MOF electrodes. For Ce-MOF, the solution resistance (*Rs*) and charge transfer resistance (*Rp*) were found to be 1.18 Ω and 3.04 Ω, respectively. In the case of GO@Ce-MOF, the Rs value further decreased to 1.14 Ω, and the *Rp* Rp value reduced to 2.9 Ω. These reductions indicate enhanced conductivity and improved charge transfer dynamics in the GO@Ce-MOF composite compared to pure Ce-MOF (Ahmed Malik *et al.*, 2022).

These findings demonstrate the role of GO in improving the electrochemical properties of Ce-MOF composites by reducing resistance and enhancing ion transport, thereby contributing to the superior performance of the material in energy storage applications.

Future Challenges

This review highlights the potential of Ce-MOF-derived composites in supercapacitors, showcasing their promising role in advancing energy storage

technologies. However, one of the primary challenges in this field is the limited availability of research focused specifically on Ce-MOFs in supercapacitor applications. Addressing this limitation requires a comprehensive exploration of related areas, such as CeO_2, graphene oxide (GO), carbon nanotube (CNT)-based materials, and other metal-organic frameworks (MOFs). These related fields provide valuable insights into synthesis methods, characterization techniques, and electrochemical studies that can guide the development of Ce-MOF composites.

As an emerging research area, the study of Ce-MOFs in supercapacitors is rapidly evolving. Supercapacitors play a crucial role in various applications, including hybrid vehicles, smartphones, and portable power sources, due to their exceptional properties such as long cycle life, fast charge-discharge rates, and high power densities. Despite these advantages, supercapacitors face inherent challenges, including high costs, lower energy density, and reduced electrical conductivity compared to batteries (Gautham Prasad *et al.*, 2019). As a result, extensive research is underway to develop materials capable of overcoming these limitations.

Ce-MOFs have shown great potential in enhancing the capacitance of supercapacitors. To further improve their electrical conductivity, incorporating reduced graphene oxide (rGO) has proven effective due to its low electrical resistance (Fatemi *et al.*, 2022). Additionally, the introduction of sulfides can enhance electron transfer among electrolyte ions. Sulfides, with lower electronegativity than oxygen, improve conductivity and hold promise as effective electrode materials for supercapacitors (Lee *et al.*, 2021; Bibi *et al.*, 2018).

Optimizing the morphology and composition of Ce-MOFs is also critical for enhancing their electrochemical performance. By precisely controlling the size, shape, and porosity of Ce-MOF particles, their specific surface area, ion accessibility, and charge transfer kinetics can be significantly improved (Zhang *et al.*, 2016). Furthermore, tuning the composition through the incorporation of functional groups or dopants can enhance their capacitive behavior. Practical considerations, such as electrode thickness, loading density, and current collector material, should also be carefully optimized to reduce resistance and ensure efficient charge transport.

The design of hierarchical or nanostructured electrodes with well-defined pores and interconnected pathways is another promising avenue for improving ion diffusion, reducing diffusion lengths, and boosting overall electrochemical performance. Such advancements could address the current limitations of supercapacitors and open new opportunities for Ce-MOF composites as effective materials for energy storage devices.

This review on Ce-MOF-derived composites in supercapacitors provides a valuable resource for researchers, offering a comprehensive understanding of the field and highlighting the opportunities and challenges ahead. By overcoming the current limitations, Ce-MOF composites could emerge as a highly effective material for supercapacitor electrodes, enabling the development of promising energy storage devices for a wide range of applications.

CONCLUSION

In conclusion, this comprehensive review provides a detailed exploration of the utilization of Ce-MOF-derived composites-specifically Ce-MOF/CeO_2, Ce-MOF/GO, and Ce-MOF/CNT-as efficient materials for supercapacitors. It underscores the critical role of supercapacitors in diverse applications and highlights the pressing need for advanced materials to overcome current limitations. Ce-MOF and its composites demonstrate immense potential due to their unique properties, including high surface area, tunable porosity, and redox activity, which make them suitable for high-performance energy storage.

The review extensively discusses the synthesis methods for Ce-MOF composites and various characterization techniques, such as XRD, SEM, TEM, XPS, and FTIR. Additionally, it examines the electrochemical performance of Ce-MOF electrodes using cyclic voltammetry (CV), galvanostatic charge-discharge (GCD), and electrochemical impedance spectroscopy (EIS). Ce-MOFs exhibit excellent electrochemical properties, including high specific capacitance, outstanding cycling stability, and rapid charge-discharge kinetics. The pseudocapacitive behavior, driven by the reversible redox reactions of cerium ions (Ce^{3+}/Ce^{4+}), significantly enhances their charge storage capabilities.

The review also emphasizes the importance of optimization strategies for Ce-MOF-derived composites in supercapacitor applications. These strategies include tailoring the morphology and composition of the composites, hybridization with other materials, electrode design optimization, and surface functionalization. By implementing these

strategies, the electrochemical performance, cycling stability, and overall energy storage capabilities of Ce-MOF electrodes can be further enhanced.

Overall, this review serves as a valuable resource for researchers, scientists, and engineers in the energy storage field. By fostering further exploration and innovation, it lays the foundation for the development of high-performance, durable, and cost-effective supercapacitors that can meet the growing energy storage demands across various sectors. applications.

Conflicts of interest

There are no conflicts to declare.

Author Contribution

Ruhani Baweja: data curation, Investigation, Methodology, Formal analysis, Writing original draft.

Sanjeev Gautam: data curation, Conceptualization, formal analysis, fund ing acquisition, investigation, Methodology, Project administration, Resources, Supervision, Validation, Visualization, writing-review & editing. ♦

REFERENCES

Abdel Maksoud, M. I. A., Fahim, R. A., Shalan, A. E., Abd Elkodous, M., Olojede, S. O., Osman, A. I., … & Rooney, D. W. (2021). Advanced materials and technologies for supercapacitors used in energy conversion and storage: a review. *Environmental Chemistry Letters, 19*, 375-439.

Abdeladim, M., & Ashraf, A. (2015). Review of Super capacitor Technology. *Int. J. Comput. Sci. Electron. Eng.(IJCSEE), 3*(3).

Agarwal, S., Burr, G., Chen, A., Das, S., Debenedictis, E., Frank, M. P., … & Rakshit, T. (2018). *International Roadmap of Devices and Systems 2017 Edition: Beyond CMOS chapter* (No. SAND2018-3550R). Sandia National Lab. (SNL-NM), Albuquerque, NM (United States).

Ahmed Malik, W. M., Afaq, S., Mahmood, A., Niu, L., Yousaf ur Rehman, M., Ibrahim, M., … & Chughtai, A. H. (2022). A facile synthesis of CeO2 from the GO@ Ce-MOF precursor and its efficient performance in the oxygen evolution reaction. *Frontiers in Chemistry, 10*, 996560.

Aiyappa, H. B., Pachfule, P., Banerjee, R., & Kurungot, S. (2013). Porous carbons from nonporous MOFs: influence of ligand characteristics on intrinsic properties of end carbon. *Crystal Growth & Design*, *13*(10), 4195-4199.

Anwer, A. H., Ansari, M. Z., Mashkoor, F., Zhu, S., Shoeb, M., & Jeong, C. (2023). Synergistic effect of carbon nanotube and tri-metallic MOF nanoarchitecture for electrochemical high-performance asymmetric supercapacitor applications and their charge storage mechanism. *Journal of Alloys and Compounds*, *955*, 170038.

Augustyn, V., Simon, P., & Dunn, B. (2014). Pseudocapacitive oxide materials for high-rate electrochemical energy storage. *Energy & Environmental Science*, *7*(5), 1597-1614.

Babu, S., Thanneeru, R., Inerbaev, T., Day, R., Masunov, A. E., Schulte, A., & Seal, S. (2009). Dopant-mediated oxygen vacancy tuning in ceria nanoparticles. *Nanotechnology*, *20*(8), 085713.

Balasubramaniam, S., Mohanty, A., Balasingam, S. K., Kim, S. J., & Ramadoss, A. (2020). Comprehensive insight into the mechanism, material selection and performance evaluation of supercapatteries. *Nano-Micro Letters*, *12*, 1-46.

Baumann, A. E., Burns, D. A., Liu, B., & Thoi, V. S. (2019). Metal-organic framework functionalization and design strategies for advanced electrochemical energy storage devices. *Communications Chemistry*, *2*(1), 86.

Bellani, S., Petroni, E., Del Rio Castillo, A. E., Curreli, N., Martín-García, B., Oropesa-Nuñez, R., … & Bonaccorso, F. (2019). Scalable production of graphene inks via wet-jet milling exfoliation for screen-printed micro-supercapacitors. *Advanced Functional Materials*, *29*(14), 1807659.

Bibi, N., Xia, Y., Ahmed, S., Zhu, Y., Zhang, S., & Iqbal, A. (2018). Highly stable mesoporous CeO2/CeS2 nanocomposite as electrode material with improved supercapacitor electrochemical performance. *Ceramics International*, *44*(18), 22262-22270.

Brownson, D. A., Figueiredo-Filho, L. C., Ji, X., Gómez-Mingot, M., Iniesta, J., Fatibello-Filho, O., … & Banks, C. E. (2013). Freestanding three-dimensional graphene foam gives rise to beneficial electrochemical signatures within non-aqueous media. *Journal of Materials Chemistry A*, *1*(19), 5962-5972.

Cai, Y., Zhang, A., Ping Feng, Y., & Zhang, C. (2011). Switching and rectification of a single light-sensitive diarylethene molecule sandwiched between graphene nanoribbons. *The Journal of chemical physics*, *135*(18).

Cao, Y., Liang, J., Li, X., Yue, L., Liu, Q., Lu, S., … & Sun, X. (2021). Recent advances in perovskite oxides as electrode materials for supercapacitors. *Chemical Communications*, *57*(19), 2343-2355.

Cao, Y., Zhao, L., Gutmann, T., Xu, Y., Dong, L., Buntkowsky, G., & Gao, F. (2018). Getting insights into the influence of crystal plane effect of shaped ceria on its catalytic performances. *The Journal of Physical Chemistry C*, *122*(35), 20402-20409.

Cao, Y., Zhao, Y., Lv, Z., Song, F., & Zhong, Q. (2015). Preparation and enhanced CO2 adsorption capacity of UiO-66/graphene oxide composites. *Journal of Industrial and Engineering Chemistry*, *27*, 102-107.

Cao, Z., Momen, R., Tao, S., Xiong, D., Song, Z., Xiao, X., … & Ji, X. (2022). Metal-organic framework materials for electrochemical supercapacitors. *Nano-micro letters*, *14*(1), 181.

Choi, K. M., Jeong, H. M., Park, J. H., Zhang, Y. B., Kang, J. K., & Yaghi, O. M. (2014). Supercapacitors of nanocrystalline metal-organic frameworks. *ACS nano*, *8*(7), 7451-7457.

Cong, H. P., Ren, X. C., Wang, P., & Yu, S. H. (2013). Flexible graphene-polyaniline composite paper for high-performance supercapacitor. *Energy & Environmental Science*, *6*(4), 1185-1191.

De Combarieu, G., Morcrette, M., Millange, F., Guillou, N., Cabana, J., Grey, C. P., … & Tarascon, J. M. (2009). Influence of the benzoquinone sorption on the structure and electrochemical performance of the MIL-53 (Fe) hybrid porous material in a lithium-ion battery. *Chemistry of Materials*, *21*(8), 1602-1611.

Dezfuli, A. S., Kohan, E., Naderi, H. R., & Salehi, E. (2019). Study of the supercapacitive activity of a Eu-MOF as an electrode material. *New Journal of Chemistry*, *43*(23), 9260-9264.

Díaz, R., Orcajo, M. G., Botas, J. A., Calleja, G., & Palma, J. (2012). Co8-MOF-5 as electrode for supercapacitors. *Materials Letters*, *68*, 126-128.

Djire, A., Pande, P., Deb, A., Siegel, J. B., Ajenifujah, O. T., He, L., … & Thompson, L. T. (2019). Unveiling the pseudocapacitive charge storage mechanisms of nanostructured vanadium nitrides using in-situ analyses. *Nano Energy*, *60*, 72-81.

Dürkop, T., Getty, S. A., Cobas, E., & Fuhrer, M. S. (2004). Extraordinary mobility in semiconducting carbon nanotubes. *Nano letters*, *4*(1), 35-39.

Elkholy, A. E., Heakal, F. E. T., & Allam, N. K. (2017). Nanostructured spinel manganese cobalt ferrite for high-performance supercapacitors. *RSC advances*, *7*(82), 51888-51895.

Ethiraj, J., Bonino, F., Vitillo, J. G., Lomachenko, K. A., Lamberti, C., Reinsch, H., … & Bordiga, S. (2016). Solvent-Driven Gate Opening in MOF-76-Ce: Effect on CO2 Adsorption. *ChemSusChem*, *9*(7), 713-719.

Faraji, S., & Ani, F. N. (2015). The development supercapacitor from activated carbon by electroless plating – A review. *Renewable and Sustainable Energy Reviews*, *42*, 823-834.

Fatemi, S., & Ganjali, M. R. (2022). Fabrication and comparison of composites of cerium metal-organic framework/reduced graphene oxide as the electrode in supercapacitor application. *Journal of Energy Storage*, *55*, 105545.

Fauzi, A. A., Jalil, A. A., Hassan, N. S., Aziz, F. F. A., Azami, M. S., Hussain, I., … & Vo, D. V. (2022). A critical review on relationship of CeO2-based photocatalyst towards mechanistic degradation of organic pollutant. *Chemosphere*, *286*, 131651.

Fleker, O., Borenstein, A., Lavi, R., Benisvy, L., Ruthstein, S., & Aurbach, D. (2016). Preparation and properties of metal organic framework/activated carbon composite materials. *Langmuir*, *32*(19), 4935-4944.

Gautam, S., Verma, M., Chauhan, R., Aghara, S., & Goyal, N. (2023). Reviewing thermal conductivity aspects of solar salt energy storage. *Energy Advances*.

Gautham Prasad, G., Shetty, N., Thakur, S., Rakshitha, & Bommegowda, K. B. (2019, October). Supercapacitor technology and its applications: a review. In *IOP Conference Series: Materials Science and Engineering* (Vol. 561, No. 1, p. 012105). IOP Publishing.

Ghosh, S., Anbalagan, K., Kumar, U. N., Thomas, T., & Rao, G. R. (2020). Ceria for supercapacitors: dopant prediction, and validation in a device. *Applied Materials Today*, *21*, 100872.

Ghosh, S., De Adhikari, A., Nath, J., Nayak, G. C., & Nayek, H. P. (2019). Lanthanide (III) Metal-Organic Frameworks: Syntheses, Structures and Supercapacitor Application. *ChemistrySelect*, *4*(36), 10624-10631.

Gonçalves, J. M., da Silva, M. I., Toma, H. E., Angnes, L., Martins, P. R., & Araki, K. (2020). Trimetallic oxides/hydroxides as hybrid supercapacitor electrode materials: a review. *Journal of Materials Chemistry A*, *8*(21), 10534-10570.

Gong, Q., Li, Y., Huang, H., Zhang, J., Gao, T., & Zhou, G. (2018). Shape-controlled synthesis of Ni-CeO2@ PANI nanocomposites and their synergetic effects on supercapacitors. *Chemical Engineering Journal, 344*, 290-298.

Green, A., & Jehoulet, C. (2002). The non-battery battery-The potential role of supercapacitors in standby power applications. In *The Battcon 2002 Proceedings.*

Halper, M. S., & Ellenbogen, J. C. (2006). *Supercapacitors: A brief overview.* The MITRE Corporation, McLean, Virginia, USA, 1.

Hassan, M. H., Andreescu, D., & Andreescu, S. (2020). Cerium oxide nanoparticles stabilized within metal-organic frameworks for the degradation of nerve agents. *ACS Applied Nano Materials, 3*(4), 3288-3294.

He, X., Looker, B. G., Dinh, K. T., Stubbs, A. W., Chen, T., Meyer, R. J., … & Dincă, M. (2020). Cerium (IV) enhances the catalytic oxidation activity of single-site Cu active sites in MOFs. *ACS Catalysis, 10*(14), 7820-7825.

Hossain, E., Faruque, H. M. R., Sunny, M. S. H., Mohammad, N., & Nawar, N. (2020). A comprehensive review on energy storage systems: Types, comparison, current scenario, applications, barriers, and potential solutions, policies, and future prospects. *Energies, 13*(14), 3651.

Hou, Q., Zhou, S., Wei, Y., Caro, J., & Wang, H. (2020). Balancing the grain boundary structure and the framework flexibility through bimetallic Metal-Organic Framework (MOF) membranes for gas separation. *Journal of the American Chemical Society, 142*(21), 9582-9586.

Huang, H., Chen, Y., Chen, Z., Chen, J., Hu, Y., & Zhu, J. J. (2021). Electrochemical sensor based on Ce-MOF/carbon nanotube composite for the simultaneous discrimination of hydroquinone and catechol. *Journal of Hazardous Materials, 416*, 125895.

Inoue, H., Morimoto, T., & Nohara, S. (2007). Electrochemical characterization of a hybrid capacitor with Zn and activated carbon electrodes. *Electrochemical and Solid-State Letters, 10*(12), A261.

Iro, Z. S., Subramani, C., & Dash, S. S. (2016). A brief review on electrode materials for supercapacitor. *International Journal of Electrochemical Science, 11*(12), 10628-10643.

Jacobsen, J., Ienco, A., D'Amato, R., Costantino, F., & Stock, N. (2020). The chemistry of Ce-based metal-organic frameworks. *Dalton Transactions, 49*(46), 16551-16586.

Jafari, H., Mohammadnezhad, P., Khalaj, Z., Naderi, H. R., Kohan, E., Hosseini, M. R. M., & Dezfuli, A. S. (2020). Terbium metal-organic frameworks as capable electrodes for supercapacitors. *New Journal of Chemistry, 44*(27), 11615-11621.

Javed, M. S., Shah, H. U., Shaheen, N., Lin, R., Qiu, M., Xie, J., … & Hu, C. (2018). High energy density hybrid supercapacitor based on 3D mesoporous cuboidal Mn2O3 and MOF-derived porous carbon polyhedrons. *Electrochimica Acta, 282*, 1-9.

Javed, N., Noor, T., Iqbal, N., & Naqvi, S. R. (2023). A review on development of metal-organic framework-derived bifunctional electrocatalysts for oxygen electrodes in metal-air batteries. *RSC advances, 13*(2), 1137-1161.

Jayakumar, A., Antony, R. P., Wang, R., & Lee, J. M. (2017). MOF-derived hollow cage NixCo3-xO4 and their synergy with graphene for outstanding supercapacitors. *Small, 13*(11), 1603102.

Jeyaranjan, A. (2020). Cerium Oxide based Nanocomposites for Supercapacitors.

Jiang, Y., & Liu, J. (2019). Definitions of pseudocapacitive materials: a brief review. *Energy & Environmental Materials, 2*(1), 30-37.

Jiao, L., Seow, J. Y. R., Skinner, W. S., Wang, Z. U., & Jiang, H. L. (2019). Metal-organic frameworks: Structures and functional applications. *Materials Today, 27*, 43-68.

Kang, L., Sun, S. X., Kong, L. B., Lang, J. W., & Luo, Y. C. (2014). Investigating metal-organic framework as a new pseudo-capacitive material for supercapacitors. *Chinese Chemical Letters, 25*(6), 957-961.

Karthikeyan, S., Narenthiran, B., Sivanantham, A., Bhatlu, L. D., & Maridurai, T. (2021). Supercapacitor: Evolution and review. *Materials Today: Proceedings, 46*, 3984-3988.

Kaur, M., Gautam, S., & Goyal, N. (2022). Ion-implantation and photovoltaics efficiency: A review. *Materials Letters, 309*, 131356.

Kaur, M., Gautam, S., Chae, K. H., Klysubun, W., & Goyal, N. (2023). Charge transfer and X-ray absorption investigations in aluminium and copper co-doped zinc oxide nanostructure for perovskite solar cell electrodes. *Scientific Reports, 13*(1), 10769.

Khan, U. A., Iqbal, N., Noor, T., Ahmad, R., Ahmad, A., Gao, J., … & Wahab, A. (2021). Cerium based metal organic framework derived

composite with reduced graphene oxide as efficient supercapacitor electrode. *Journal of Energy Storage, 41*, 102999.

Kowsuki, K., Nirmala, R., Ra, Y. H., & Navamathavan, R. (2023). Recent advances in cerium oxide-based nanocomposites in synthesis, characterization, and energy storage applications: A comprehensive review. *Results in Chemistry, 5*, 100877.

Lammert, M., Wharmby, M. T., Smolders, S., Bueken, B., Lieb, A., Lomachenko, K. A., … & Stock, N. (2015). Cerium-based metal organic frameworks with UiO-66 architecture: synthesis, properties and redox catalytic activity. *Chemical Communications, 51*(63), 12578-12581.

Lee, C. S., Lim, J. M., Park, J. T., & Kim, J. H. (2021). Direct growth of highly organized, 2D ultra-thin nano-accordion Ni-MOF@ NiS2@ C core-shell for high performance energy storage device. *Chemical Engineering Journal, 406*, 126810.

Lee, D. Y., Yoon, S. J., Shrestha, N. K., Lee, S. H., Ahn, H., & Han, S. H. (2012). Unusual energy storage and charge retention in Co-based metal-organic-frameworks. *Microporous and Mesoporous Materials, 153*, 163-165.

Li, C., Hu, C., Zhao, Y., Song, L., Zhang, J., Huang, R., & Qu, L. (2014). Decoration of graphene network with metal-organic frameworks for enhanced electrochemical capacitive behavior. *Carbon, 78*, 231-242.

Li, C., Zhang, X., Lv, Z., Wang, K., Sun, X., Chen, X., & Ma, Y. (2021). Scalable combustion synthesis of graphene-welded activated carbon for high-performance supercapacitors. *Chemical Engineering Journal, 414*, 128781.

Li, H., Li, Z., Sun, M., Wu, Z., Shen, W., & Fu, Y. Q. (2019). Zinc cobalt sulfide nanoparticles as high performance electrode material for asymmetric supercapacitor. *Electrochimica Acta, 319*, 716-726.

Li, K., Teng, H., Dai, X., Wang, Y., Wang, D., Zhang, X., … & Zhang, Y. (2022). Atomic scale modulation strategies and crystal phase transition of flower-like CoAl layered double hydroxides for supercapacitors. *CrystEngComm, 24*(11), 2081-2088.

Li, X., Tang, Y., Song, J., Yang, W., Wang, M., Zhu, C., … & Lin, Y. (2018). Self-supporting activated carbon/carbon nanotube/reduced graphene oxide flexible electrode for high performance supercapacitor. *Carbon, 129*, 236-244.

Li, Y., Ma, L., Yi, Z., Zhao, Y., Mao, J., Yang, S., … & Kim, J. K. (2021). Metal-organic framework-derived carbon as a positive electrode for high-performance vanadium redox flow batteries. *Journal of Materials Chemistry A*, 9(9), 5648-5656.

Liang, J., Huang, Y., Oh, J., Kozlov, M., Sui, D., Fang, S., … & Chen, Y. (2011). Electromechanical actuators based on graphene and graphene/Fe3O4 hybrid paper. *Advanced Functional Materials, 21*(19), 3778-3784.

Libich, J., Máca, J., Vondrák, J., Čech, O., & Sedlaříková, M. (2018). Supercapacitors: Properties and applications. *Journal of Energy Storage, 17*, 224-227.

Lin, J., Yan, Y., Wang, H., Zheng, X., Jiang, Z., Wang, Y., … & Feng, J. (2019). Hierarchical Fe2O3 and NiO nanotube arrays as advanced anode and cathode electrodes for high-performance asymmetric supercapacitors. *Journal of Alloys and Compounds, 794*, 255-260.

Liu, H., & Le, Q. (2016). Synthesis and performance of cerium oxide as anode materials for lithium ion batteries by a chemical precipitation method. *Journal of Alloys and Compounds, 669*, 1-7.

Liu, N., Tang, Q., Huang, B., & Wang, Y. (2021). Graphene synthesis: method, exfoliation mechanism and large-scale production. *Crystals, 12*(1), 25.

Liu, T., Zhang, L., You, W., & Yu, J. (2018). Core-shell nitrogen-doped carbon hollow spheres/Co3O4 nanosheets as advanced electrode for high-performance supercapacitor. *Small, 14*(12), 1702407.

Lu, G., Li, S., Guo, Z., Farha, O. K., Hauser, B. G., Qi, X., … & Huo, F. (2012). Imparting functionality to a metal-organic framework material by controlled nanoparticle encapsulation. *Nature Chemistry, 4*(4), 310-316.

Lu, T., Zhang, Y., Li, H., Pan, L., Li, Y., & Sun, Z. (2010). Electrochemical behaviors of graphene-ZnO and graphene-SnO2 composite films for supercapacitors. *Electrochimica Acta, 55*(13), 4170-4173.

Maheswari, N., & Muralidharan, G. (2015). Supercapacitor behavior of cerium oxide nanoparticles in neutral aqueous electrolytes. *Energy & Fuels, 29*(12), 8246-8253.

Maiti, S., Pramanik, A., & Mahanty, S. (2014). Extraordinarily high pseudocapacitance of metal organic framework derived nanostructured cerium oxide. *Chemical Communications, 50*(79), 11717-11720.

Matsuda, Y., Tahir-Kheli, J., & Goddard III, W. A. (2010). Definitive band gaps for single-wall carbon nanotubes. *The Journal of Physical Chemistry Letters, 1*(19), 2946-2950.

Mehtab, T., Yasin, G., Arif, M., Shakeel, M., Korai, R. M., Nadeem, M., … & Lu, X. (2019). Metal-organic frameworks for energy storage devices: Batteries and supercapacitors. *Journal of Energy Storage, 21*, 632-646.

Meng, X., Wan, C., Jiang, X., & Ju, X. (2018). Rod-like CeO 2/carbon nanocomposite derived from metal-organic frameworks for enhanced supercapacitor applications. *Journal of Materials Science, 53*, 13966-13975.

Mishra, S. R., & Ahmaruzzaman, M. (2021). Cerium oxide and its nanocomposites: structure, synthesis, and wastewater treatment applications. *Materials Today Communications, 28*, 102562.

Mohanty, A., Jaihindh, D., Fu, Y. P., Senanayak, S. P., Mende, L. S., & Ramadoss, A. (2021). An extensive review on three dimension architectural Metal-Organic Frameworks towards supercapacitor application. *Journal of Power Sources, 488*, 229444.

Montini, T., Melchionna, M., Monai, M., & Fornasiero, P. (2016). Fundamentals and catalytic applications of CeO2-based materials. *Chemical Reviews, 116*(10), 5987-6041.

Muzaffar, A., Ahamed, M. B., Deshmukh, K., & Thirumalai, J. (2019). A review on recent advances in hybrid supercapacitors: Design, fabrication and applications. *Renewable and Sustainable Energy Reviews*, 101, 123-145.

Nikolaidis, P., & Poullikkas, A. (2017). A comparative review of electrical energy storage systems for better sustainability. *Journal of Power Technologies, 97*(3), 220-245.

Padmanathan, N., & Selladurai, S. (2014). Shape controlled synthesis of CeO2 nanostructures for high performance supercapacitor electrodes. *RSC Advances, 4*(13), 6527-6534.

Peigney, A., Laurent, C., Flahaut, E., Bacsa, R. R., & Rousset, A. (2001). Specific surface area of carbon nanotubes and bundles of carbon nanotubes. *Carbon, 39*(4), 507-514.

Peng, M. M., Ganesh, M., Vinodh, R., Palanichamy, M., & Jang, H. T. (2019). Solvent free oxidation of ethylbenzene over Ce-BTC MOF. *Arabian Journal of Chemistry, 12*(7), 1358-1364.

Ponnaiah, S. K., & Prakash, P. (2021). A new high-performance supercapacitor electrode of strategically integrated cerium vanadium oxide and polypyrrole nanocomposite. International *Journal of Hydrogen Energy, 46*(37), 19323-19337.

Prasanna, K., Subburaj, T., Jo, Y. N., Lee, W. J., & Lee, C. W. (2015). Environment-friendly cathodes using biopolymer chitosan with enhanced electrochemical behavior for use in lithium ion batteries. *ACS Applied Materials & Interfaces, 7*(15), 7884-7890.

Pujar, M. S., Hunagund, S. M., Barretto, D. A., Desai, V. R., Patil, S., Vootla, S. K., & Sidarai, A. H. (2020). Synthesis of cerium-oxide NPs and their surface morphology effect on biological activities. *Bulletin of Materials Science, 43*(1), 24.

Qu, C., Zhang, L., Meng, W., Liang, Z., Zhu, B., Dang, D., … & Zou, R. (2018). MOF-derived α-NiS nanorods on graphene as an electrode for high-energy-density supercapacitors. *Journal of Materials Chemistry A, 6*(9), 4003-4012.

Ramachandran, R., Saranya, M., Kollu, P., Raghupathy, B. P., Jeong, S. K., & Grace, A. N. (2015). Solvothermal synthesis of Zinc sulfide decorated Graphene (ZnS/G) nanocomposites for novel Supercapacitor electrodes. *Electrochimica Acta, 178*, 647-657.

Ramachandran, R., Xuan, W., Zhao, C., Leng, X., Sun, D., Luo, D., & Wang, F. (2018). Enhanced electrochemical properties of cerium metal-organic framework based composite electrodes for high-performance supercapacitor application. *RSC advances, 8*(7), 3462-3469.

Ramineni, P., Pandian, A., Kumar, M. K., & Sundaram, K. M. (2022). Improved operation of Li-ion battery with supercapacitor realized to solar-electric vehicle. *Energy Reports, 8*, 256-264.

Raptopoulou, C. P. (2021). Metal-Organic Frameworks: Synthetic Methods and Potential Applications. *Materials 2021, 14, 310.*

Raza, W., Ali, F., Raza, N., Luo, Y., Kim, K. H., Yang, J., … & Kwon, E. E. (2018). Recent advancements in supercapacitor technology. *Nano Energy, 52*, 441-473.

Raza, W., Nabi, G., Shahzad, A., Malik, N., & Raza, N. (2021). Electrochemical performance of lanthanum cerium ferrite nanoparticles for supercapacitor applications. Journal of Materials Science: *Materials in Electronics, 32*, 7443-7454.

Redondo, E., Le Fevre, L. W., Fields, R., Todd, R., Forsyth, A. J., & Dryfe, R. A. (2020). Enhancing supercapacitor energy density by

mass-balancing of graphene composite electrodes. Electrochimica Acta, 360, 136957.

Riaz, A., Sarker, M. R., Saad, M. H. M., & Mohamed, R. (2021). Review on comparison of different energy storage technologies used in micro-energy harvesting, WSNs, low-cost microelectronic devices: challenges and recommendations. *Sensors*, *21*(15), 5041.

Şahin, M. E., Blaabjerg, F., & Sangwongwanich, A. (2022). A Comprehensive Review on Supercapacitor Applications and Developments. *Energies 2022*, *15*, *674*.

Sangeetha, S., & Krishnamurthy, G. (2020). Electrochemical and photocatalytic applications of Ce-MOF. *Bulletin of Materials Science*, *43*(1), 269.

Saraf, M., Rajak, R., & Mobin, S. M. (2016). A fascinating multitasking Cu-MOF/rGO hybrid for high performance supercapacitors and highly sensitive and selective electrochemical nitrite sensors. *Journal of Materials Chemistry A*, *4*(42), 16432-16445.

Shah, V. A., Joshi, J. A., Maheshwari, R., & Roy, R. (2008, December). Review of ultracapacitor technology and its applications. In *Proceedings of the 15th National Power System Conference* (pp. 142-147).

Sharma, K., Arora, A., & Tripathi, S. K. (2019). Review of supercapacitors: Materials and devices. *Journal of Energy Storage*, *21*, 801-825.

Sharma, P., & Kumar, V. (2020). Current technology of supercapacitors: A review. *Journal of Electronic Materials*, *49*(6), 3520-3532.

Shen, C. H., Chuang, C. H., Gu, Y. J., Ho, W. H., Song, Y. D., Chen, Y. C., … & Kung, C. W. (2021). Cerium-based metal-organic framework nanocrystals interconnected by carbon nanotubes for boosting electrochemical capacitor performance. *ACS Applied Materials & Interfaces*, *13*(14), 16418-16426.

Sinan, N., & Unur, E. (2016). Fe3O4/carbon nanocomposite: Investigation of capacitive & magnetic properties for supercapacitor applications. *Materials Chemistry and Physics*, *183*, 571-579.

Smith, K. A. (2010). Electrochemical control of lithium-ion batteries [applications of control]. *IEEE Control Systems Magazine*, *30*(2), 18-25.

Snook, G. A., Kao, P., & Best, A. S. (2011). Conducting-polymer-based supercapacitor devices and electrodes. *Journal of Power Sources*, *196*(1), 1-12.

Song, H., Shen, L., Wang, J., & Wang, C. (2016). Reversible lithiation-delithiation chemistry in cobalt based metal organic framework nanowire electrode engineering for advanced lithium-ion batteries. Journal of Materials Chemistry A, 4(40), 15411-15419.

Song, M. K., Park, S., Alamgir, F. M., Cho, J., & Liu, M. (2011). Nanostructured electrodes for lithium-ion and lithium-air batteries: the latest developments, challenges, and perspectives. *Materials Science and Engineering: R: Reports*, *72*(11), 203-252.

Stock, N., & Biswas, S. (2012). Synthesis of metal-organic frameworks (MOFs): routes to various MOF topologies, morphologies, and composites. *Chemical Reviews*, *112*(2), 933-969.

Su, L. H., Zhang, X. G., Mi, C. H., Gao, B., & Liu, Y. (2009). Improvement of the capacitive performances for Co-Al layered double hydroxide by adding hexacyanoferrate into the electrolyte. *Physical Chemistry Chemical Physics*, *11*(13), 2195-2202.

Subramanian, G., & Peter, J. (2020, July). Integrated Li-ion battery and super capacitor based hybrid energy storage system for electric vehicles. In *2020 IEEE International Conference on Electronics, Computing and Communication Technologies (CONECCT)* (pp. 1-6). IEEE.

Tang, Z., Pei, Z., Wang, Z., Li, H., Zeng, J., Ruan, Z., … & Zhi, C. (2018). Highly anisotropic, multichannel wood carbon with optimized heteroatom doping for supercapacitor and oxygen reduction reaction. *Carbon*, *130*, 532-543.

Teffu, D. M. (2021). *Palladium-reduced graphene oxide/metal organic framework as an efficient electrode material for battery-type supercapacitor applications* (Doctoral dissertation).

Tiwari, S. K., Sahoo, S., Wang, N., & Huczko, A. (2020). Graphene research and their outputs: Status and prospect. *Journal of Science: Advanced Materials and Devices*, *5*(1), 10-29.

van Voorden, A. M., Elizondo, L. M. R., Paap, G. C., Verboomen, J., & van der Sluis, L. (2007, July). The application of super capacitors to relieve battery-storage systems in autonomous renewable energy systems. In *2007 IEEE Lausanne Power Tech* (pp. 479-484). IEEE.

Varghese, J., Wang, H., & Pilon, L. (2011). Simulating electric double layer capacitance of mesoporous electrodes with cylindrical pores. *Journal of The Electrochemical Society*, *158*(10), A1106.

Venkataraman, A., Amadi, E. V., Chen, Y., & Papadopoulos, C. (2019). Carbon nanotube assembly

and integration for applications. *Nanoscale Research Letters, 14*, 1-47.

Walkey, C., Das, S., Seal, S., Erlichman, J., Heckman, K., Ghibelli, L., … & Self, W. T. (2015). Catalytic properties and biomedical applications of cerium oxide nanoparticles. *Environmental Science: Nano, 2*(1), 33-53.

Wang, G., Zhang, L., & Zhang, J. (2012). A review of electrode materials for electrochemical supercapacitors. *Chemical Society Reviews, 41*(2), 797-828.

Wang, L., Feng, X., Ren, L., Piao, Q., Zhong, J., Wang, Y., … & Wang, B. (2015). Flexible solid-state supercapacitor based on a metal-organic framework interwoven by electrochemically-deposited PANI. *Journal of the American Chemical Society, 137*(15), 4920-4923.

Wang, L., Han, Y., Feng, X., Zhou, J., Qi, P., & Wang, B. (2016). Metal-organic frameworks for energy storage: Batteries and supercapacitors. *Coordination Chemistry Reviews, 307*, 361-381.

Wang, Q., Jiao, L., Du, H., Si, Y., Wang, Y., & Yuan, H. (2012). Co 3 S 4 hollow nanospheres grown on graphene as advanced electrode materials for supercapacitors. *Journal of Materials Chemistry, 22*(40), 21387-21391.

Wang, Q., Jiao, L., Du, H., Wang, Y., & Yuan, H. (2014). Fe3O4 nanoparticles grown on graphene as advanced electrode materials for supercapacitors. *Journal of Power Sources, 245*, 101-106.

Wang, T., Chen, H. C., Yu, F., Zhao, X. S., & Wang, H. (2019). Boosting the cycling stability of transition metal compounds-based supercapacitors. *Energy Storage Materials, 16*, 545-573.

Wang, Y. (2008). *Modeling of ultracapacitor short-term and long-term dynamic behavior* (Master's thesis, University of Akron).

Wang, Y., Liu, Y., Wang, H., Liu, W., Li, Y., Zhang, J., … & Yang, J. (2019). Ultrathin NiCo-MOF nanosheets for high-performance supercapacitor electrodes. ACS *Applied Energy Materials, 2*(3), 2063-2071.

Wang, Y., Wang, X., Dai, X., Li, K., Bao, Z., Li, H., … & Zhang, Y. (2021). Structural evolution and sulfuration of nickel cobalt hydroxides from 2D to 1D on 3D diatomite for supercapacitors. *CrystEngComm, 23*(33), 5636-5644.

Wang, Z., Zhao, K., Lu, S., & Xu, W. (2020). Application of flammulina-velutipes-like CeO2/Co3O4/rGO in high-performance asymmetric supercapacitors. *Electrochimica Acta, 353*, 136599.

Wen, P., Gong, P., Sun, J., Wang, J., & Yang, S. (2015). Design and synthesis of Ni-MOF/CNT composites and rGO/carbon nitride composites for an asymmetric supercapacitor with high energy and power density. *Journal of Materials Chemistry A, 3*(26), 13874-13883.

Xia, J., Chen, F., Li, J., & Tao, N. (2009). Measurement of the quantum capacitance of graphene. *Nature Nanotechnology, 4*(8), 505-509.

Xie, S., Wang, Z., Cheng, F., Zhang, P., Mai, W., & Tong, Y. (2017). Ceria and ceria-based nanostructured materials for photoenergy applications. *Nano Energy, 34*, 313-337.

Xu, B., Zhang, H., Mei, H., & Sun, D. (2020). Recent progress in metal-organic framework-based supercapacitor electrode materials. *Coordination Chemistry Reviews, 420*, 213438.

Xu, J., Wang, K., Zu, S. Z., Han, B. H., & Wei, Z. (2010). Hierarchical nanocomposites of polyaniline nanowire arrays on graphene oxide sheets with synergistic effect for energy storage. *ACS nano, 4*(9), 5019-5026.

Yan, J., Fan, Z., Wei, T., Qian, W., Zhang, M., & Wei, F. (2010). Fast and reversible surface redox reaction of graphene-MnO2 composites as supercapacitor electrodes. *Carbon, 48*(13), 3825-3833.

Yang, G., Zhang, D., Zhu, G., Zhou, T., Song, M., Qu, L., … & Li, H. (2020). A Sm-MOF/GO nanocomposite membrane for efficient organic dye removal from wastewater. *RSC Advances, 10*(14), 8540-8547.

Yang, J., Ma, Z., Gao, W., & Wei, M. (2017). Layered structural co-based MOF with conductive network frames as a new supercapacitor electrode. *Chemistry – A European Journal, 23*(3), 631-636.

Yang, J., Zheng, C., Xiong, P., Li, Y., & Wei, M. (2014). Zn-doped Ni-MOF material with a high supercapacitive performance. J*ournal of Materials Chemistry A, 2*(44), 19005-19010.

Yang, Q., Liu, W., Wang, B., Zhang, W., Zeng, X., Zhang, C., … & Lu, J. (2017). Regulating the spatial distribution of metal nanoparticles within metal-organic frameworks to enhance catalytic efficiency. *Nature Communications, 8*(1), 14429.

Yang, Q., Wang, Q., Long, Y., Wang, F., Wu, L., Pan, J., … & Song, S. (2020). In situ formation of Co9S8 quantum dots in MOF-derived ternary metal layered double hydroxide nanoarrays for high-performance hybrid supercapacitors. *Advanced Energy Materials, 10*(7), 1903193.

Yang, Q., Xu, Q., & Jiang, H. L. (2017). Metal-organic frameworks meet metal nanoparticles: synergistic effect for enhanced catalysis. *Chemical Society Reviews*, *46*(15), 4774-4808.

Yang, W., Gao, Z., Song, N., Zhang, Y., Yang, Y., & Wang, J. (2014). Synthesis of hollow polyaniline nano-capsules and their supercapacitor application. *Journal of Power Sources*, *272*, 915-921.

Yuan, C., Zhang, X., Su, L., Gao, B., & Shen, L. (2009). Facile synthesis and self-assembly of hierarchical porous NiO nano/micro spherical superstructures for high performance supercapacitors. *Journal of Materials Chemistry*, *19*(32), 5772-5777.

Yuan, J., Wang, B. Y., Zong, Y. C., & Zhang, F. Q. (2023). Ce-MOF modified Ceria-based photocatalyst for enhancing the photocatalytic performance. *Inorganic Chemistry Communications*, *153*, 110799.

Zang, X., Zhang, R., Zhen, Z., Lai, W., Yang, C., Kang, F., & Zhu, H. (2017). Flexible, temperature-tolerant supercapacitor based on hybrid carbon film electrodes. *Nano Energy*, *40*, 224-232.

Zeng, G., Chen, Y., Chen, L., Xiong, P., & Wei, M. (2016). Hierarchical cerium oxide derived from metal-organic frameworks for high performance supercapacitor electrodes. *Electrochimica Acta*, *222*, 773-780.

Zhang, Q., & Deng, W. (2016). An adaptive energy management system for electric vehicles based on driving cycle identification and wavelet transform. *Energies*, *9*(5), 341.

Zhang, W., Yang, L. P., Wu, Z. X., Piao, J. Y., Cao, A. M., & Wan, L. J. (2016). Controlled formation of uniform CeO 2 nanoshells in a buffer solution. *Chemical Communications*, *52*(7), 1420-1423.

Zhao, J., & Burke, A. F. (2021). Review on supercapacitors: Technologies and performance evaluation. *Journal of Energy Chemistry*, *59*, 276-291.

Zhao, Y., Song, Z., Li, X., Sun, Q., Cheng, N., Lawes, S., & Sun, X. (2016). Metal organic frameworks for energy storage and conversion. *Energy Storage Materials*, *2*, 35-62.